**ICRA2010**

**2010 IEEE International Conference on Robotics and Automation**
**Anchorage, Alaska USA**
**May 3-8, 2010**

# Signals Measurement and Estimation Techniques Issues in the Micro/Nano-World

**Full-day Workshop, May 3 2009**

**Cédric Clévy**
**Micky Rakotondrabe**
**Nicolas Chaillet**

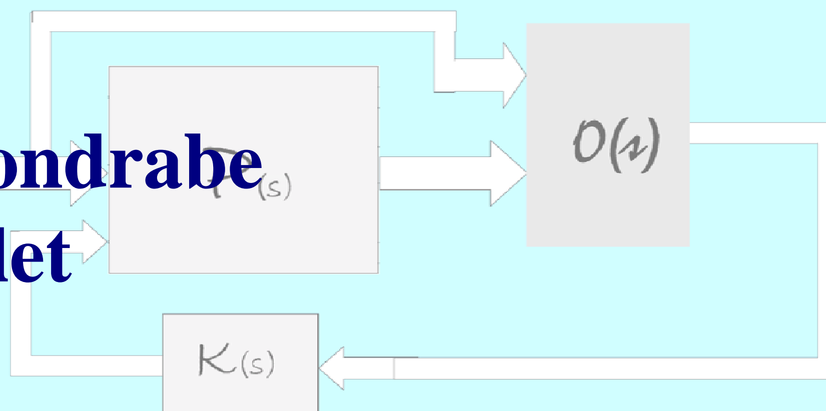

# *Workshop Contents*


Introduction **1**

Observer techniques applied to the control of piezoelectric microactuators **3**
***Micky Rakotondrabe, Cédric Clévy, Ioan Alexandru Ivan and Nicolas Chaillet***

Measurement and control for high-speed sub-atomic positioning in scanning probe microscopes **10**
***Andrew J. Fleming and Kam K. Leang***

Microrobotic tools for the measurement of small forces **16**
***S. Muntwyler, F. Beyele and B. J. Nelson***

In situ characterizations of thin-film nanostructures with large-range direct force sensing **19**
***Gilgueng Hwang and Stéphane Régnier***

In-situ mechanical characterization of mouse oocytes using a cell holding device **22**
***Xinyu Liu, Roxanne Fernander, Andrea Jurisicova, Robert F. Casper and Yu Sun***

Observer-based estimation of weak forces in a nanosystem measurement device **24**
***Alina Voda and Gildas Besançon***

A mechanism approach for enhancing the dynamic range and linearity of MEMS optical force sensing **29**
***Gloria J. Wiens***

# *Introduction*

The need of high performances micro/nano robots and microrobotic cells increases rapidly. These new technologies can be used for applications such as micromanipulation (artificial components, biological objects), micro-assembly (MEMS, MOEMS, NEMS), material and surface force characterization. At the micro/nano scales, sensing is a key issue to control systems and to understand physical phenomena. Numerous sensors with suitable resolution and range are necessarily required.

Positioning accuracy and resolution have to be in the submicrometer range while those concerning force are in the micro-nano Newton range. Moreover, some applications require high dynamic performances and then high bandwidth sensors, for instance the automation of piezoelectric based micromanipulation robots. On the one hand, sensors that guarantee these performances are bulky and expensive (interferometers, scanning electron microscopes, cameras, laser sensors). Furthermore, most of these sensors generally enable only one or 2D measurements. On the other hand, sensors that are compact and convenient for packaging (strain gage, piezoceramic sensor, etc.) are very fragile and have very limited performance and robustness.

To overcome these limitations, several approaches can be used: observation/estimation techniques which require less sensors or indirect ones, development of a new generation of sensors thanks to recent and fast progresses of microfabrication techniques and sensors technologies. Self-sensing methods using active materials also currently know fast development. The objective of this workshop is to present recent results on these topics.

The main objectives of this workshop is to provide an overview of the recent measurement systems and signal estimation techniques performed for robots dedicated to act in the micro/nano world. The information concerned in this workshop is mainly force and position. At these scales, force and position signal are commonly of very small amplitude and exhibit a small signal/noise ratio. Nevertheless, the integration of sensors with suitable performances (high bandwidth, very high accuracy and convenient size, integration ability) remains highly challenging. In fact, it appears that the lack of such sensors is the main limitation to successfully perform the control of robots in the micro/nano world and to push back the limits of automation, as for example required in rapid and precise microassembly. These last years, the technological obstacles have led researchers to the design of a new generation of integrated sensors (Silicon/PZT, etc.), self-sensing methods in active materials and advanced signal estimation coming from control theory.

**Cédric Clévy,**
**Micky Rakotondrabe,**
**Nicolas Chaillet.**

Automatic Control and Micro-Mechatronic Systems Department (AS2M),
FEMTO-st Institute,
UMR CNRS 6174 - UFC / ENSMM / UTBM
24, rue Alain Savary
25000 Besançon – FRANCE

# Observer Techniques Applied to the Control of Piezoelectric Microactuators

Micky Rakotondrabe, *Member, IEEE,* Cédric Clévy, *Member, IEEE,*
Ioan Alexandru Ivan, *Member, IEEE,* and Nicolas Chaillet, *Member, IEEE,*

***Abstract*— We present here the use of sensors, observers and self-sensing techniques to control piezoelectric actuators, particularly piezocantielevers.**

**First, the feedback control with full measurements (all variables are measured) is presented. Because of the lack of convenient sensors for the microworld, non-full measurements combined with observer techniques is proposed. Finally, the self-sensing principle, where the actuator is at the same time sensor, is applied and used for the feedback.**

## I. Introduction

The need of high performances micro/nano robots and systems increases rapidly. These new technologies can be used for applications such as micromanipulation (of artificial components and biological objects), microassembly (of MEMS, MOEMS, NEMS), material and surface force characterization, biological analysis, etc. At the micro/nano scales, sensing is a key issue to control systems and to understand physical phenomena. Numerous sensors with suitable resolution and range are necessarily required.

This paper give a survey on the sensing and measurement possibilities for microsystems. We particularly focus on piezoelectric based actuator with cantilevered structure. The concern variables are the displacement and the force.

Section II introduces the main but very influent specificities of the microscale. Current technical and physical limitations are explained and consequences on micro/nano robots and systems are given. Several state of the art solutions are investigated including these specificities. Section III introduces the full measurement, i.e. where sensors display direct and suitable measured information, and its use to the control of piezoelectric actuators. When direct measurement is not available, observers are required. Several applications of observer techniques for piezoelectric actuators are introduced in Section IV. Finally, we present the self-sensing technique where the piezoelectric actuator is also the sensing element. In this case, no external sensor is necessary. However, an electronic circuit followed by a convenient observer scheme is used to provide the estimate force and/or the displacement. This technique is presented in Section V.

FEMTO-st Institute,
UMR CNRS-6174 / UFC / ENSMM / UTBM
Automatic Control and Micro-Mechatronic Systems department (AS2M department)
25000 Besançon - France
{mrakoton, cclevy, alex.ivan, nicolas.chaillet}@femto-st.fr

## II. Microscales specificities

Micro/nano robots and systems require specific studies and developments. Indeed, the down scaling greatly influences the required specifications for and the behavior of robots and systems. For example, assembly of human sized systems is generally done by hand for technico-economical optimization reasons whereas assembly of microsized components requires robotized systems assistance. Thus, the development of automated microassembly systems constitutes a key issue in the development of new micro-assembled products which is not the case at the macro scale [1]. Microscale systems or systems acting at the microscale therefore require the integration of actuators and sensors.

At the microscale, systems have to achieve positioning accuracy and resolution in the submicrometer range and forces in the micro-nano Newton range. Moreover, some applications require high dynamic performances and then high bandwidth sensors, for instance the automation of piezoelectric based micromanipulation robots. Unfortunately, sensors that guarantee these performances are bulky and expensive (interferometers, scanning electron microscopes, cameras, laser sensors). Furthermore, most of these sensors generally enable only one or 2D measurements. On the other hand, sensors that are compact and convenient for packaging (strain gage, piezoceramic sensor, etc.) are very fragile and have very limited performances and robustness. In addition, scaling down decrease signal to noise ratio. Specific studies to understand the sources of noises and to find solutions to take them into account become of great importance. Moreover, surface force becomes predominant at the microscale. For example, they can reach 200 $\mu$N for 50x50 $\mu N^2$ planar contacts [2]. These forces are for the most influent, capillary pull-off and van der Waals forces. The lack of models, knowledge and experimentations at the microscale is a source of great difficulties for applications like micromanipulation and microassembly [3].

All of these microscale specificities therefore require developments of new sensors and sensing principles taking into account suitable range, resolution, free space, and dynamic [4].

## III. Presentation of the piezoelectric actuators used in this paper

In the sequel, we are interested by the measurement/observation and control of displacement and force in piezoelectric cantilevers (piezocantilevers) especially dedicated to micromanipulation and microassembly tasks, where the range of displacement is up to some hundred of $\mu m$ and the range of force up to several tens of $mN$. Cantilevered piezoelectric actuators are used in different applications: AFM-piezotubes, microgrippers, tweezers, stepper (stick-slip and inch-worm) microrobots, etc. Even if we use a unimorph piezocantilever with rectangular section in this paper, the techniques can be applied to other cantilevers.

A unimorph piezocantilever is made up of one piezoelectric layer, often Lead Zirconate Titanate (PZT) ceramic, and one passive layer. Commonly used passive layers is Nickel. When applying a voltage $U$ to the piezolayer, it expands/contracts resulting a global deflection $\delta$ of the cantilever (Fig. 1). Furthermore, a force $F$ applied at its tip also results a deflection.

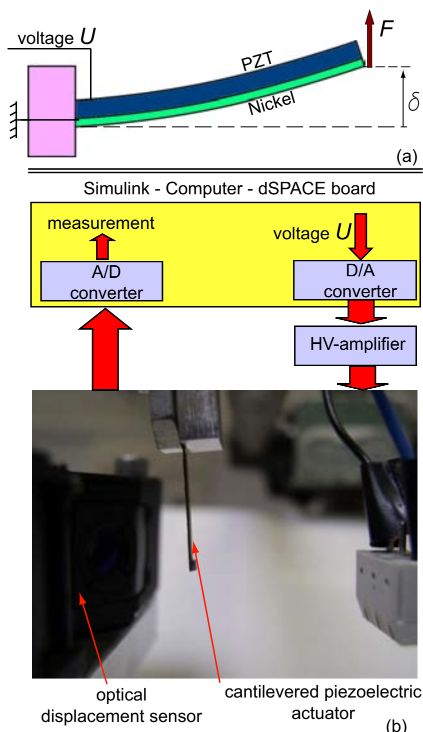


Fig. 1. A unimorph piezoelectric cantilever.

## IV. Full measurement and control applications

We mean by full measurement the fact that all suitable signals used for the feedback control are directly measured by sensors. The main part of this section is to give a survey of sensors that can be used to control piezoelectric based actuators, especially piezocantilevers.

### A. Existing sensors

*1) Pinpoint measurement:* they concern measurement that measure one point of the actuator. To measure the displacement $\delta$, optical displacement sensors are very common (Fig. 1-b). It can offer up to $10nm$ of resolution and $\pm 150\mu m$ of range [5]. If the tasks need a higher resolution and range, an interferometer measurement system can be the solution. For applications which require the force control, femto-tools force sensors are adapted [6].

*2) Vision-based measurement:* despite the high resolution of the optical and the femto-tools sensors, they are limited to measure one point of the actuator. So, they could not be used to search the location of the object when there is not yet contact between the latter and the actuator, or when the contact point has changed. To surpass this limitation, vision based measurement have been used [7]. This technique can measure both the location of the object and the displacement/deformation of the actuator.

The main disadvantages of the optical, the vision based measurement and the femto-tools sensors are their bulky sizes and their relatively high costs. As a result, they are not adapted for packaged high performances microsystems. This is why embarked sensors have been developed. They are cited below.

*3) Strain gauges:* they are glued on the surface of the piezoelectric cantilever and the displacement or force at its tip is easily deduced. The offered resolution and the accuracy depend on the number of the used gauges, of the quality of the Wheatstone bridge and of the electronic amplifier. Thanks to the low costs and the small sizes of strain gauges, they have been used in numerous applications in the field of micromanipulation and microassembly [8][9][10]. Finally, *Arai et al.* developed multi-axis strain gauges dedicated to complex micromanipulation [11]. The main disadvantages of strain gauges are their fragility and their high sensitivity to noises.

*4) Piezoelectric sensors:* it consists in putting two couples of electrodes on the surfaces of the piezocantilever. While one couple is used to supply the voltage input for the actuation, the second one is used to measure the output charge for the displacement/force sensing. These sensors provide a high bandwidth [12]. However, they are not adapted to static measurement because of the drift (creep) characteristics [13]. Piezoelectric sensors can be based on classical piezoelectric materials such as PZT [14][15] or PVDF (PolyVinylidine DiFluoride) [16][17].

*5) Capacitive sensors:* an alternative way of embarked sensors is based on the capacitive principle. Similarly to the piezoelectric sensor, it can be designed and developed with the same bulk than the actuator. In fact, the sensing element and the actuation element are made of the same material making them very adapted to microfabrication techniques [18].

*6) Piezomagnetic sensors:* these sensors are based on transducers whose the magnetization changes when a

mechanical stress is applied [12]. An example of piezomagnetic sensor is given in [19].

### B. Commonly used control techniques

Because the measurement (displacement or force) constitutes the variable to be controlled, output feedback with controllers in cascade are often designed (Fig. 2-a). They ranges from PID structure with a trial and error tuning to advanced $H_\infty$ control laws, with or without accounting the nonlinearities in the piezoelectric actuators [20][21][22]. The results (Fig. 2-b) are convenient to the specifications required in micromanipulation and microassembly, such as micrometric accuracy and some tens of millisecond of settling time.

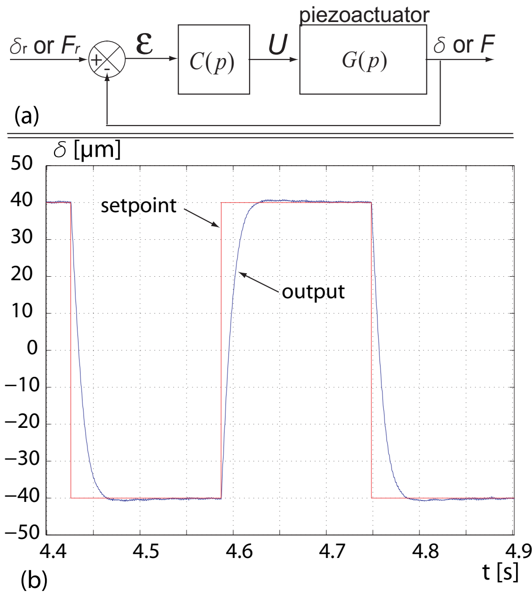


Fig. 2. (a) bloc scheme of the output feedback control using controllers in cascade. (b) a series of step response of the closed-loop.

### C. Limitation of the used sensors

On the one hand, high accuracy sensors are expensive and bulky (optical, interferometer, etc.). On the other hand, small sensors are fragile and very sensitive to noises (strain gauges, etc.). Furthermore, some applications necessitate the measurement of both displacement and force during the tasks, as example during a pick-and-place task, and therefore necessitate many sensors.

In order to gain space and to go to the packageability of the microsystems, two approaches were proposed: 1) the use of small sensors (strain gauges) and the rejection of the noises using the Kalman filtering, 2) the use of reduced number of sensors and the application of observers to complete the measurement. The next section is focused on these points.

## V. Observers and non-full measurement

In this section, we consider that one or more variables used for the feedback is not directly measured. The use of observer techniques is therefore advised.

Reconsider the piezocantilever presented in Fig. 1. The model linking the input voltage $U$, the force $F$ applied at the tip and the output deflection $\delta$, in the linear case, is:

$$\delta = d_p.U.D(s) + s_p.F.D(s) \qquad (1)$$

where $d_p$ and $s_p$ are the piezoelectric and the elastic coefficients respectively, and $D(s)$ (with $D(0) = 1$) is the dynamic part.

When the applied electrical field -through the voltage $U$- is high, the nonlinearities behavior of the piezoelectric materials becomes nonnegligible. These nonlinearities are the hysteresis and the creep and need to be taken into account when applying an observer. The nonlinear model of the actuator is therefore [21]:

$$\delta = H(U).D(s) + C_r(s).U + s_p.F.D(s) \qquad (2)$$

where $H(\cdot)$ is an operator that describes the (static) hysteresis and $C_r(s)$ is a linear approximation of the creep.

### A. Strain gauges sensors, Kalman filtering and state feedback control

In [23], strain gauges were used to measure the deflection $\delta$ of the piezocantilever with a view to reduce the sizes of the whole microsystems (actuators and sensors). To reduce the noises of the measured signals, the authors apply a Kalman filtering computed with the linear model (equ 1). In addition to the noises rejection, the technique allows the estimation of the states of the system and therefore allows the use of state feedback control techniques (Fig. 3).

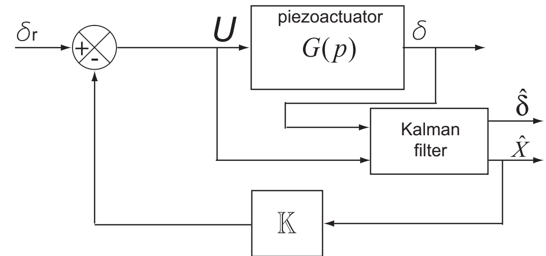


Fig. 3. Measurement of $\delta$ with strain gauges and use of a Kalman filter.

### B. Force estimation using the Luenberger observer

In [24], two piezocantilevers forming a microgripper were used. While one piezocantilever is used to accurately position the manipulated object, the second one is used only to estimate the manipulation force (Fig. 4-a). To estimate the input force, the latter has been considered as a state of the system. Because a derivative is required in the state equation, the author considers the condition $\frac{dF}{dt} = 0$. As a result, the state vector is composed of the deflection $\delta$, its derivative $\frac{d\delta}{dt}$ and the force $F$. Based on the model in (equ 1), a Luenberger observer has been applied (Fig. 4-b).

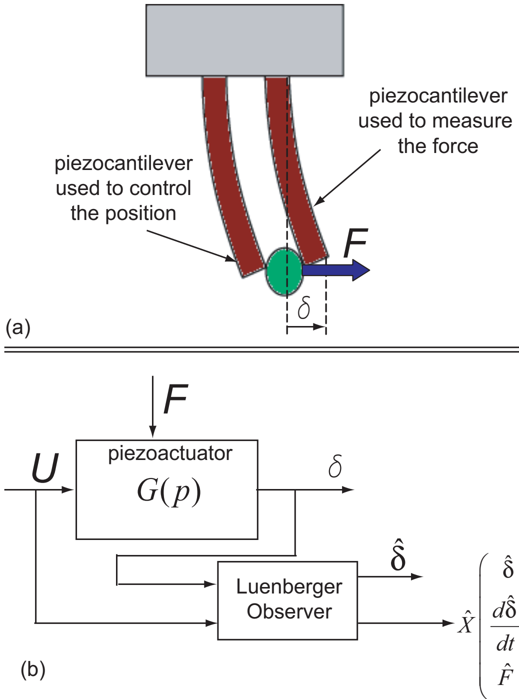


Fig. 4. (a) use of one piezocantilever of the microgripper to estimate the manipulation force. (b) estimation of the force using the Luenberger observer.

### C. Force estimation and Unknown Input Observer technique (UIO)

When the force is considered as a state to be estimated, it requires that the dynamics model of the force is known. In the previous case, the derivative of $F$ has been considered to be null and the estimation was only valuable for static case. It has also been demonstrated that the dynamics of the force in piezocantilevers always depend on the characteristics of the manipulated object [25]. Therefore, considering the force as a state is not convenient if the estimate will be used in a control purpose. This is why the Unkown Input Observer techinque (UIO) has been proposed recently [26]. The Inverse-Dynamics-Based UIO technique [27] was especially applied. In this, we consider the force as an unknown input. A classical observer is first employed to estimate the state vector (composed of the deflection and its derivative). Afterwards, a second observer is applied to estimate the force (Fig. 5).

### D. Force estimation in the nonlinear case, open loop Observer

In [28], another approach was proposed to estimate the force. It consists in using the nonlinear model in (equ 2)) and directly deducing the force:

$$\hat{F} = \frac{1}{s_p.D(s)} \left(\delta - H\left(U\right).D(s) - C_r\left(s\right).U\right) \qquad (3)$$

where the hysteresis $H(\cdot)$ was modeled by the Bouc-Wen approach.

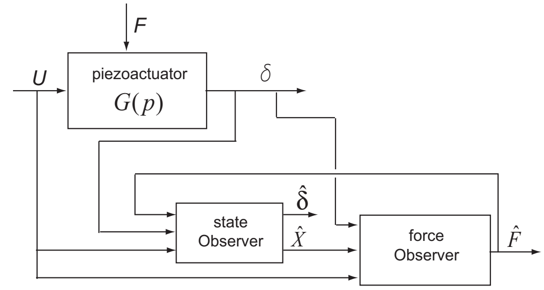


Fig. 5. Inverse-Dynamics-Based UIO technique to estimate the unknown input force.

This method requires the bistability of $D(s)$ as its inverse is used in the (open-loop) observer. If the system is linear, the method can also be applied. Indeed, the term $d_pU$ of (equ 1)) is a linear approximation of the hysteresis term $H(\cdot)$ in (equ 2)), the creep $C_r(s)$ being set to zero.

As presented in Fig. 6, the observer has an open-loop structure, and therefore is sensitive to model uncertainty.

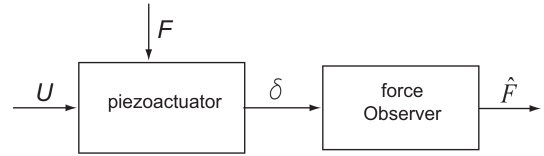


Fig. 6. Nonlinear open-loop observer.

### E. Application to control

The Luenberger observer for the estimation of $\delta$ and $\frac{d\delta}{dt}$ was successfully used in a state feedback control law of the displacement [24]. References [25][29][30] used successfully the nonlinear open-loop observer to estimate the force and to apply $H_\infty$ based controllers.

## VI. Self-sensing based control

As shown above, accurate sensors are often bulky and expensive while integrable ones are fragile and not robust. There exist an alternate, simple and cost-effective up-grade solution for most types of existing piezoelectric actuators: the self-sensing technique.

### A. Principle of the self-sensing

It consists in using the actuator as also the sensor. The principle is as follows. When a voltage $U$ and/or an external force $F$ are applied to the piezocantilever, it bends. Charges $Q$ also appear at its surface. Using a charge amplifier (electronic circuit) and a convenient observer, it is possible to estimate both the dipslacement and the force [41]. This "intrinsic technique" can therefore be used in a closed-loop system without needing external sensors.

Often charge measurement is rejected on false idea that PZT is a very bad isolating material. In fact, not the leaking resistivity, which is high enough for preserving

charges (hundreds of seconds) but ferroelectric material non-linearities (hysteresis, creep) or the temperature influence put the challenge on the charge-based self-sensing.

### B. Historical of the self-sensing

The first use of "self-sensing" term dates back to 1992 when *Dosch et al.* [31] successfully damped the vibration of a piezoelectric beam without the aid of external sensors. Voltage drop provided from a capacitive bridge was processed in an analog circuit, amplified and returned back to the piezoelectric element. Soon, several independent applications began to emerge for beam vibration control or micropositioning of piezo stacks. Several years later *Takigami et al.* [32] applied the method to force self-sensing and control a large size bimorph actuator, using a half-bridge circuit, a voltage follower and PC-based data acquisition system. They experimentally shown that the stiffness of the manipulated object does not affect the measurement. However, the electronic circuit limited the applied voltage range and the nonlinearities (hysteresis and creep) of the piezoelectric element were not compensated.

A self-sensing based on integrator electronic circuit was introduced in [33] focusing on a compounding control of displacement combining a PID feedback control with a feedforward control of hysteretic behavior. Self-sensing force control for piezo stack was introduced in [34][35]. In the latter paper, the hysteresis nonlinearity was taken into account by using the generalized Maxwell-slip hysteresis operator [36]. As a result, the static displacement error was reported to 2 to 4% while static force error is nearly 5%. In [37], a modified bridge electronic circuit with adaptable gain was intended for vibration control under structural deformation. In [38], self-sensing technique was used to ameliorate the positioning and vibration in hard-disk drives. Finally, in [39], the use of self-sensing microdispensing system shows better positioning performance than the use of external sensors.

Other sensorless methods close to self-sensing concept consist in shaping several electrodes on the actuator and dedicating them separately for actuation or sensing [14] (see also the *Section-IV.4. Piezoelectric sensor*). The drawback is that a fraction of the actuation capability is lost. However, the nonlinear effects are avoided and signals are well separated. More recently a SPM piezotube scanner with a new electrode pattern allowed self-measurement of nanometer resolution with improved transfer function in the observer [40].

### C. Static displacement/force self-sensing

Most of the above papers focused on short-term (less than 1s) displacement and/or force self-sensing control or vibration damping. Until our recent works ([41] for the displacement self-sensing, [42] for the displacement and force self-sensing), there was a lack of publications related to long term self-sensing of piezoelectric cantilevers intended for microsystems manipulation. In quasistatic (low frequency) regime, the electric charge over the electrodes of the uni- or bimorph piezocantilever is intrinsically proportional to the free displacement. The main ferroelectric nonlinearities (hysteresis, creep) are automatically included. Thus, there is no need to compensate the hysteresis and creep of the actuators. The electronic circuit and the observer presented in [41](Fig. 7) relies on the current integration and compensation of the second-degree nonlinearities such as PZT leaking resistance, bias currents and dielectric absorption. The temperature influences was also discussed in the paper, and the attained accuracy was 0.5% over a period of 600 seconds. In [42] we reported the simultaneous force-displacement self-sensing of the piezo cantilever entering in contact with an object. For that purpose, we modeled the nonlinear behaviour of the free actuator (including hysteresis and creep operators) and fused the result with the electronic signal, deriving the estimate force and displacement.

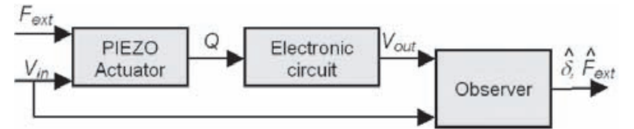


Fig. 7. Generic principle of a self-sensing system [41].

### D. Dynamic displacement self-sensing

The method proposed in [41] was upgraded in [28] in order to complete the static displacent self-sensing by the dynamic part (Fig. 8). The estimate signal can be therefore used control applications.

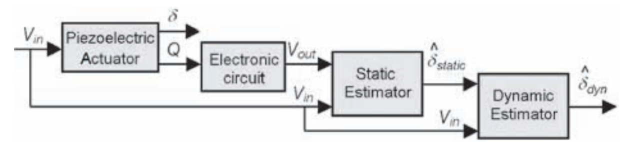


Fig. 8. Extension of the static self-sensing in [41] to dynamic self-sensing [28].

### E. Discussion

To sum up, the first advantage of self-sensing is the cost, external sensors not being needed anymore. System will be more flexible in terms of space occupation, allowing better miniaturization and dexterity in terms of DoF. Also, actuators dynamics will no longer be affected by mechanically attached sensors (e.g. strain gages or micromangnets). Number of connecting cables will be reduced. Disadvantages consist in adding a supplementary electronic circuit (but of reduced complexity). Electronic circuit is based on a capacitive bridge (or divider) or a current integrator. Specific applications with dedicated electrodes for sensing (such as in *Section-IV.4. Piezoelectric sensor*) may measure directly strain-induced voltage. Attention has to be paid for preserving the charge as

long as possible. Non-linearities such as hysteresis and creep due to ferroelectric domain relaxation put the most challenge on self-sensing technique, limiting its accuracy, especially in force sensing. Identifying these nonlinear effects requires an extra procedure. Finally, temperature influence, noise or other uncertainties may prevent the system to attain required accuracy or resolution.

## VII. Conclusion

This paper presented the different methods that have been used to measure, observe and sense the signals (especially force and displacement) in piezoelectric actuators and particularly piezocantilevers.

We first presented the existing sensors that can be used. They offer a full-measurement based control applications. Afterwards, we shown that observers can be used to complete the measurement when some signals are not directly measured. Finally, the self-sensing techniques - that can be applied when no sensor is available- were presented and end the paper.

## References


[1] D. O. Popa, R. Murthy, and A. N. Das 'M3 - Deterministic, Multiscale, Multirobot Platform for Microsystems Packaging: Design and Quasi-Static Precision Evaluation' IEEE Transaction on Automation Science and Engineering, 2009 , 6 , 345-61

[2] K. Rabenorosoa, C. Clévy, P. Lutz, M. Gauthier and P. Rougeot 'Measurement setup of pull-off force for planar contact at the microscale' Micro-nano letters, vol(4), Issue(3), pp:148-154, septembre 2009

[3] M. Gauthier, S. Regnier, P. Rougeot and N. Chaillet ŚForces analysis for micromanipulations in dry and liquid mediaŠ, J. Micromechatronics, 2006, 3, pp. 389Ű413

[4] F. Beyeler, S. Muntwyler, and B.J. Nelson, 'Design and Calibration of a Microfabricated 6-Axis Force-Torque Sensor for Microrobotic Applications', IEEE ICRA (International Conference on Robotics and Automation), 2009.

[5] http://www.keyence.fr/

[6] http://www.femtotools.com/

[7] Y. H. Anis, J. K. Mills and W. L. Cleghorn, 'Visual measurement of mems microassembly forces using template matching', IEEE ICRA (International Conference on Robotics and Automation), 2006.

[8] M. Goldfarb and N. Celanovic, 'A flexure-based gripper for small-scale manipulation', Robotica, 17, 1999.

[9] A. Menciassi, A. Eisinberg, M. C. Carrozza and P. Dario, 'Force sensing microinstrument for measuring tissue properties and pulse in microsurgery', IEEE/ASME Transactions on Mechatronics, 2003.

[10] P. Berkelman, L. L. Whitcomb, R. H. Taylor and P. Jensen, 'A miniature microsurgical instrument tip force sensor for enhanced force feedback during robot-assisted manipulation', IEEE Transactions on Robotics and Automation, 2003.

[11] F. Arai, A. Kawaji, T. Sugiyama, Y. Onomura, M. Ogawa, T. Fukuda, H. Iwata and K. Itoigawa, '3d micromanipulation system under microscope', IEEE International Symposium on Micromechatronics and Human Science, 1998.

[12] M. Motamed and J. Yan, 'A review of biological, biomimetic and miniature force sensing for microflight', IEEE IROS, 2005.

[13] C. K. M. Fung, I. Elhajj, W. J. Li and N. Xi, 'A 2-d pvdf force sensing system for micromanipulation and microassembly', IEEE ICRA, 2002.

[14] D. Campolo, R. Sahai and R. S. Fearing, 'Development of piezoelectric bending actuators with embedded piezoelectric sensors for micromechanical flapping mechanisms', IEEE ICRA, 2003.

[15] K. Motoo, F. Arai, Y. Yamada, T. Fukuda, T. Matsuno and H. Matsura, 'Novel force sensor using vibrating piezoelectric element', IEEE ICRA, 2005.

[16] D-H. Kim, B. Kim, S-M. Kim and H. Kang, 'Development of a piezoelectric polymer-based sensorized microgripper for microassembly and micromanipulation', IEEE IROS, 2003.

[17] A. Shen, N. Xi, C. A. Poumeroy, U. C. Wejinya and W. J. Li, 'An active micro-force sensing system with piezoelectric servomechanism', IEEE IROS, 2005.

[18] Y. Sun, B. J. Nelson, D. Potasek and E. Enikov, 'A bulk microfabricated multi-axis capacitive cellular force sensor using transverse comb drive', Journal of Micromechanics and Microengineering, 2002.

[19] M. Lohndorf, T. Zuenas-Lockwood, A. Ludwig, M. Ruhrig, D. Burgler, P. Grunberg and E. Quandt, 'A novel strain sensors based on magnetostrictive gmr/tmr structures', IEEE International Magnetics Conference, 2002.

[20] M. Rakotondrabe, C. Clévy and P. Lutz, 'H-inf deflection control of a unimorph piezoelectric cantilever under thermal disturbance', IEEE/RSJ - IROS, (International Conference on Intelligent Robots and Systems), pp:1190-1197, San Diego CA USA, Oct-Nov 2007.

[21] M. Rakotondrabe, Y. Haddab and P. Lutz, 'Quadrilateral modelling and robust control of a nonlinear piezoelectric cantilever', IEEE - Transactions on Control Systems Technology (T-CST), Vol.17, Issue 3, pp:528-539, May 2009.

[22] M. Rakotondrabe, J. Agnus, K. Rabenorosoa and N. Chaillet, 'Characterization, modeling and robust control of a nonlinear 2-dof piezocantilever for micromanipulation/microassembly', IEEE/RSJ - IROS, (International Conference on Intelligent Robots and Systems), pp:767-774, St Louis MO USA, October

[23] Y. Haddab, Q. Chen and P. Lutz, 'Improvement of strain gauges micro-forces measurement using Kalman optimal filtering.', IFAC Mechatronics, 19(4), 2009.

[24] Y. Haddab. 'Conception et réalisation dŠun système de micromanipulation contrôlé en effort et en position pour la manipulation dŠobjets de taille micrométrique'. PhD dissertation (in French), University of Franche-Comté, Laboratoire dŠautomatique de Besancon, 2000.

[25] Micky Rakotondrabe, Yassine Haddab and Philippe Lutz, 'Modelling and H-inf force control of a nonlinear piezoelectric cantilever', IEEE/RSJ - IROS, (International Conference on Intelligent Robots and Systems), pp:3131-3136, San Diego CA USA, Oct-Nov 2007.

[26] M. Rakotondrabe and P. Lutz, 'Force estimation in a piezoelectric cantilever using the inverse-dynamics-based UIO technique', IEEE - ICRA, (International Conference on Robotics and Automation), pp:2205-2210, Kobe Japan, May 2009.

[27] C-S. Liu and H. Peng, 'Inverse-dynamics based state and disturbance observers for linear time-invariant systems', ASME Journal of Dynamics Systems, Measurement and Control, vol.124, pp.375-381, September 2002.

[28] M. Rakotondrabe, I. A. Ivan, S. Khadraoui, C. Clevy, P. Lutz, and N.Chaillet, 'Dynamic Displacement Self-Sensing and Robust Control of Cantilevered Piezoelectric Actuators Dedicated to Microassembly Tasks', Submitted in IEEE/ASME AIM (Advanced Intelligent Mechatronics), 2010.

[29] M. Rakotondrabe, C. Clévy and P. Lutz, 'Modelling and robust position/force control of a piezoelectric microgripper', IEEE - CASE, (International Conference on Automation Science and Engineering), pp:39-44, Scottsdale AZ USA, Sept 2007.

[30] M. Rakotondrabe and Y. Le Gorrec, 'Force control in piezoelectric microactuators using self scheduled $H_\infty$ technique', ASME Dynamic Systems and Control Conference and IFAC Symposium on Mechatronic Systems, MIT 2010.

[31] J. J. Dosch et al., "A Self-Sensing Piezoelectric Actuator for Collocated Control", J. of Intell. Mater. Syst. and Struct., vol 3, pp. 166-185, 1992.

[32] T. Takigami et al., "Application of self-sensing actuator to control of a soft-handling gripper", Proc. to IEEE ICCA, pp. 902-906, Italy, 1998.

[33] Y. Cui et al. " Self-sensing compounding control of piezoceramic micro-motion worktable based on integrator", Proc. to 6th World Cong. On Intell. Con. and Autom., China, 2006.

[34] A. Badel et al. "Self sensing force control of a piezoelectric actuator", IEEE Trans. on UFFC, vol. 55, no. 12 Pp. 2571-2581, 2008.

[35] A. Badel et al., "Self-sensing high speed controller for piezoelectric actuator", J. of Intell. Mater. Syst. and Struct., vol 19, no. 3, pp. 395-405, 2008.

[36] M. Goldfarb and N. Celanovic, " Modeling piezoelectric stack actuators for control of micromanipulation", IEEE Control Systems Magazine, vol.3, no.3, pp.69-79, 1997.

[37] W.W. Law, W-H. Liao and J. Huang, "Vibration control of structures with self-sensing piezoelectric actuators incorporating adaptive mechanisms", Smart Mater. Struct 12, pp. 720-730, 2003.

[38] C. K. Pang et al., " Self-sensing actuation for nanopositioning and active-mode damping in dual-stage HDDs", IEEE/ASME Trans. on Mechatronics, vol. 11, no. 3, pp. 328-338, 2006.

[39] A. S. Putra et al., " With Adaptive Control in Applications With Switching Trajectory" , IEEE/ASME Trans. on Mechatronics, vol. 13, no. 1, pp. 104-110, 2008.

[40] S. O. R. Moheimani and Y. K. Yong, "Simultaneous sensing and actuation with a piezoelectric tube scanner", Review of Scientific Instruments 79, 073702, 2008

[41] I. A. Ivan, M.Rakotondrabe, P. Lutz and N. Chaillet, "Quasistatic displacement self-sensing method for cantilevered piezoelectric actuators", Review of Scientific Instruments (RSI), Vol.80(6), 065102, June 2009.

[42] I. A. Ivan, M.Rakotondrabe, P. Lutz and N. Chaillet, "Current integration force and displacement self-sensing method for cantilevered piezoelectric actuators", Review of Scientific Instruments (RSI), Vol.80(12), 2126103, December 2009.

# Measurement and Control for High-Speed Sub-Atomic Positioning in Scanning Probe Microscopes

Andrew J. Fleming and Kam K. Leang

*Abstract*— **Scanning probe microscopes require the control of position to within sub-atomic resolution. This workshop presentation will begin with an overview of the challenges and limitations encountered when attempting to achieve such resolution. This will be followed by an introduction to new measurement technologies and control techniques recently developed for high-speed nano- and micro-positioning systems, with application to scanning probe microscopy and fabrication.**

## I. INTRODUCTION

Scanning Probe Microscopes (SPMs) record localized physical interactions between a probe and sample as a function of position. A diverse range of techniques and probes have become available to image properties such as topography, electrical and mechanical forces, chemical bonding and biological interactions [1]–[5].

The positioning of the SPM probe tip relative to the sample is achieved with two basic configurations: (a) scan-by-sample or (b) scan-by-probe as shown in Figure 1. In the scan-by-sample configuration, the nanopositioner, such as the flexure-based design shown equipped with three piezo stacks, moves the sample relative to a fixed SPM probe. The $x$ and $y$ axis piezos position the sample along the lateral direction (parallel to the sample surface); a $z$ axis stack moves the sample vertically. The deflection of the cantilever is measured optically, by reflecting a laser beam off the end of the cantilever onto a nearby photodetector.

Precision positioning is a key requirement in all AFM applications. In particular, precise position control in both the lateral and vertical directions is required to hold the probe at a desired location or to track a desired motion trajectory. For instance, when the AFM is used to indent nanofeatures on a semiconductor surface to create quantum dots (2-80 nm in size), accurate position control of the indenter tip is needed because the probe position error directly affects the size, spacing, and distribution of the nanofeatures. Even 2-4 nanometers variation in size and spacing of the nanofeatures can drastically alter their properties [6]. Additionally, high-speed control of the probe's movement is needed for high throughput fabrication, imaging, and metrology. Without accurate motion control along a specific trajectory at high speed, oscillations can cause the tip to collide with nearby features, which leads to excessive tip-to-sample forces. The large forces can damage the tool tip or soft specimens such as cells. Therefore, accurate output tracking, or positioning, is critical in AFM.

Due to their high speed, compact size and essentially infinite resolution, piezoelectric actuators are used almost exclusively in scanning probe microscopes. SPM scanners and vertical positioners are usually constructed from either piezoelectric tube actuators [7], [8] or faster piezoelectric stack actuators [9]. Although scanners constructed from piezoelectric actuators have extremely high resolution, the overall accuracy is limited by creep and hysteresis [10]. For example, the positioning error due to hysteresis in a piezoelectric tube actuator has been reported to be $\pm 9.7\%$ of the scan-range [11]. This implies a maximum positioning error of almost 20% between the forward and backward scanning paths.

To avoid imaging artifacts, SPM's require some form of compensation for positioning non-linearity. Methods to accomplish this, including feedback and feedforward control, and the associated measurement and estimation problems are discussed in the following sections.

## II. HIGH-SPEED LOW-NOISE POSITION MEASUREMENT, ESTIMATION AND CONTROL

The most most popular technique for control of piezoelectric actuated systems is sensor-based feedback control with an integral or proportional-integral controller. This approach is simple, robust to modeling error, and effectively reduces non-linearity at low-frequencies. However, the bandwidth of such systems is severely limited by low gain-margin [12]. It can be shown that the maximum closed-loop bandwidth is equal to the product of twice the damping ratio $\xi$ and natural frequency $\omega_n$ [13], that is,

$$\text{max. closed-loop bandwidth} < 2\omega_n\xi. \qquad (1)$$

This is a severe limitation as the damping ratio is usually in the order of 0.01, so the maximum closed-loop bandwidth is less than 2% of the resonance frequency. Techniques aimed at improving the closed-loop bandwidth are based on either inversion of resonant dynamics using a notch filter [14] or a damping controller [15]–[18]. Damping controllers are less sensitive to variations in resonance frequency than inversion based controllers but an integral tracking loop is still required. This inevitably results in low stability margins and instability if the resonance frequency is sufficiently reduced. In addition, the greater bandwidth of damping and inversion based controllers increases the amount of positioning noise.

This work was supported by the Australian Research Council Discovery Project (DP0986319) and the Center for Complex Dynamic Systems and Control.

A. J. Fleming is with the School of Electrical Engineering and Computer Science, University of Newcastle, Callaghan, NSW 2308, Australia andrew.fleming@newcastle.edu.au

K. K. Leang is with the Department of Mechanical Engineering University of Nevada - Reno, Reno NV 89557, USA kam@unr.edu

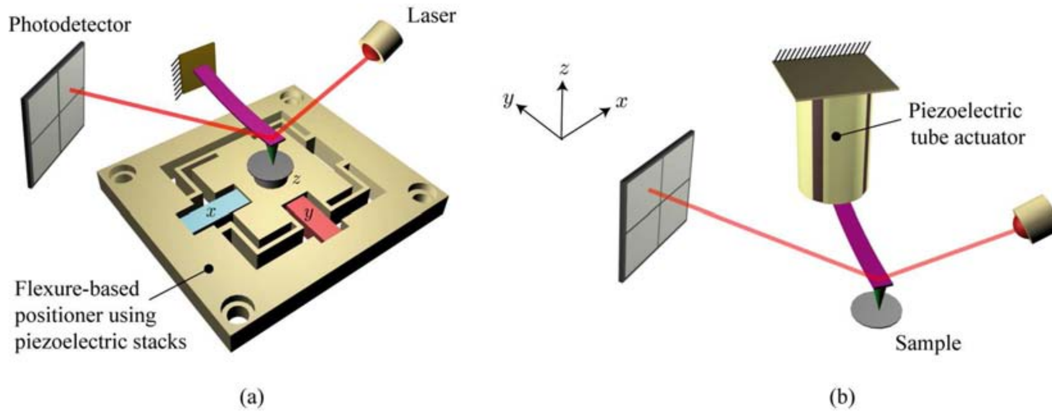


Fig. 1. Two positioning schemes for SPMs: (a) scan-by-sample and (b) scan-by-probe.

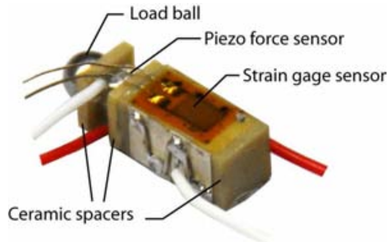


Fig. 2. A piezoelectric actuator with integrated strain and force sensors. The strain sensors are bonded to the front and back surface while the force sensor is a small piezoelectric stack placed between the actuator and load ball. The load half-ball is used to eliminate the transmission of torsion and bending moments to the force sensor and moving platform.

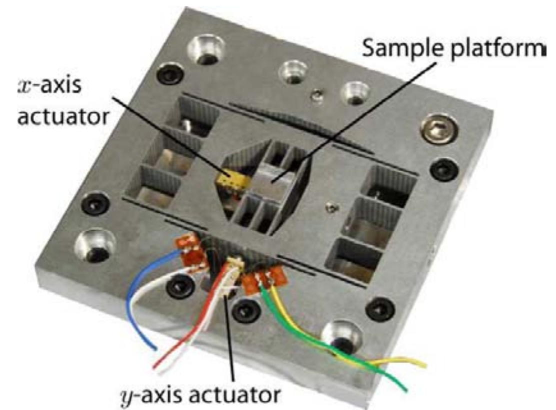


Fig. 3. High-speed nanopositioning platform with strain and force sensors fitted to the y-axis actuator.

To demonstrate the limitations imposed by sensor noise, consider a nanopositioner with feedback control derived from a capacitive sensor with a noise density of 20 pm/$\sqrt{\text{Hz}}$. An estimate of the RMS position noise can be found from the noise density and square-root of closed-loop bandwidth,

$$\text{RMS Noise} = \sqrt{3.14 \times \text{Bandwidth}} \times \text{Noise Density}, \quad (2)$$

where $3.14$ is a correction factor to convert the 3 dB bandwidth of a first-order system to an equivalent noise bandwidth. For example, with a closed-loop bandwidth of 1.8 kHz, the positioning noise is 1.5 nm RMS. If the noise is normally distributed, the $6\sigma$ peak-to-peak noise will be approximately 10 nm.

In this work, a new technique is presented for control of hysteresis, creep and vibration in piezoelectric actuated systems. As pictured in Figure 2 and 3, the proposed technique utilizes a resistive strain gage and piezoelectric force sensor to estimate displacement. The piezoelectric force sensor exhibits extremely low noise at frequencies in the Hz range and above but cannot measure static displacement and is prone to drift. To eliminate low-frequency errors, an estimator or strain gage measurement is utilized at these frequencies.

The measurement noise of the proposed piezoelectric sensor is compared to a resistive strain gage and inductive sensor in Figure 4. The superior noise performance of the piezoelectric sensor is evident. The noise density is more than two orders of magnitude lesser than the strain and inductive sensors at 100 Hz. The noise density also continues to reduce at higher frequencies.

In addition to low noise, another benefit of the piezoelectric force sensor is the zero-pole ordering of the transfer function from applied actuator voltage to measured force. This allows a simple integral controller to provide excellent tracking and damping performance with guaranteed stability.

The proposed technique of strain and force feedback was applied to the high-speed nanopositioning platform pictured in Figure 3. The closed-loop frequency response demonstrated a 33 dB damping of the resonance peak and a closed-loop bandwidth of 1.8 kHz which is close to the open-loop resonance frequency of 2.4 kHz. In the time domain, excellent tracking of a 130 Hz triangle wave is demonstrated in Figure 5. Hysteresis was reduced from 8.5% to 0.46% at 10 Hz. Although the strain gage contributes the majority of closed-loop positioning noise, the bandwidth of this signal is only 10 Hz. This resulted in a closed-loop noise of approximately 0.67 nm peak-to-peak which is 0.0067% of the 10 $\mu$m range.

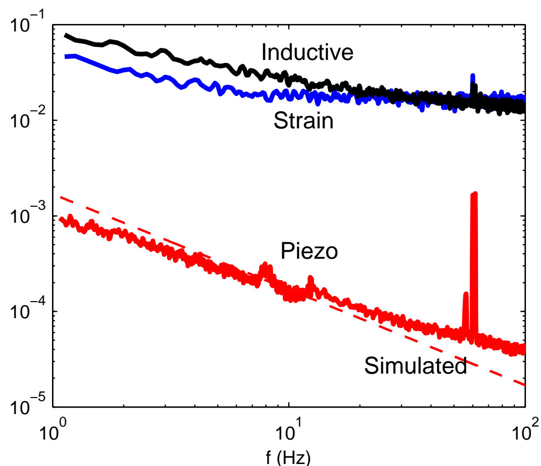


Fig. 4. The noise density of the inductive, resistive strain, and piezoelectric force sensor, all scaled to nm/$\sqrt{\text{Hz}}$. The simulated noise of the piezoelectric force sensor is also plotted as a dashed line.

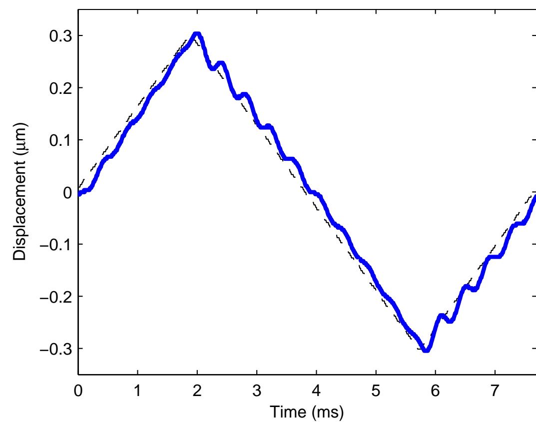


(a) Open-loop

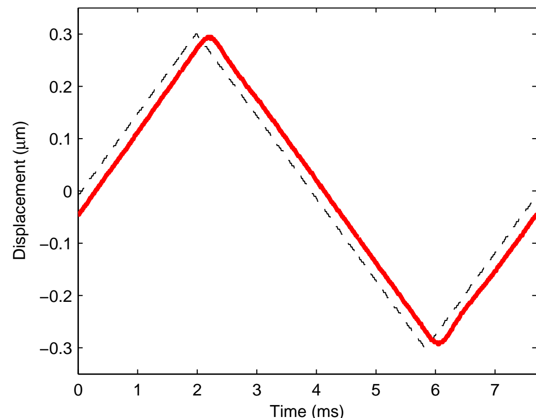


(b) Closed-loop

Fig. 5. The open- and closed-loop response to a 600 nm peak-to-peak 130 Hz triangle wave. The RMS deviation from linear over a half period was 10 nm RMS in open-loop and 1.9 nm RMS in closed-loop. The maximum peak-to-peak error over 90% of a half period was 45 nm in open-loop and 6.7 nm in closed-loop.

## III. FEEDFORWARD CONTROL

Unlike feedback control, which reacts to the measured tracking error, feedforward control compensates or anticipates for deficit performance, such as dynamic and hysteresis effects in nanopositioning systems. The feedforward approach exploits some information about the system, and thus a well-designed feedforward controller requires sufficient knowledge of the plant dynamics and nonlinearities. As shown in Figure 6(a), an inverse model produces the feedforward input $u_{ff}$ that is applied to the nanopositioning system. The effectiveness of feedforward control, that is how close the actual output $y$ matches the desired output $y_d$, depends on the *quality* of the inverse model and whether external disturbances are present. Being an open-loop approach, model uncertainty is often a challenge in feedforward control; however, the advantages often outweigh the disadvantages for applications that include high-speed scanning probe microscopy [19], [20]. In particular, feedforward control can provide high-bandwidth positioning, with performance that exceeds that of feedback-based methods [21], [22]. For robustness, feedforward control can be integrated with feedback control [23]. The integrated approach also eliminates the need for modeling and inverting nonlinear behaviors, a task that may be difficult and computationally demanding. Also, feedforward control does not require continuous sensor feedback, and thus sensor-noise related issues can be avoided entirely.

The input-output behavior of a nanopositioning system can be quite complex, consisting of structural dynamics and nonlinearities, such as hysteresis. A popular model that describes the dynamics and nonlinearity in a piezoactuator is the cascade model as depicted in Figure 6(b) [19], [24]. To determine a feedforward input for precision output tracking, each submodel is inverted as illustrated in Figure 6(c).

The inversion-based method presented above may yield excessively large inputs when the system has lightly damped system zeros. These large inputs can saturate the voltage amplifiers that drive the piezoactuator, or, even worse, depole the piezoactuator. Additionally, large model uncertainties around the resonant peaks or lightly damped zeros can cause significant error in computing the feedforward input. These model uncertainties thus lead to a lack of robustness when the inversion-based feedforward method is used. To overcome these issues, an optimal feedforward input is obtained by minimizing a quadratic cost function [25]. By choosing the frequency-dependent weights $R(j\omega)$ and $Q(j\omega)$, it is possible to systematically consider the effects of the input magnitude and the model uncertainties. For instance, the input energy weight $R(j\omega)$ can be chosen to be much larger than the tracking error weight $Q(j\omega)$ at frequencies where large model uncertainties exist or around lightly damped zeros. For details and implementation issues, see [26], [27].

To handle the hysteresis nonlinearity using the feedforward approach, the Preisach and Prandtl-Ishlinskii models are considered. These models are based on the assumption that the output is a weighted sum of elementary relays [28], [29].

Feedforward control of hysteresis and dynamics is required for long-range, high-speed nanopositioning. In this

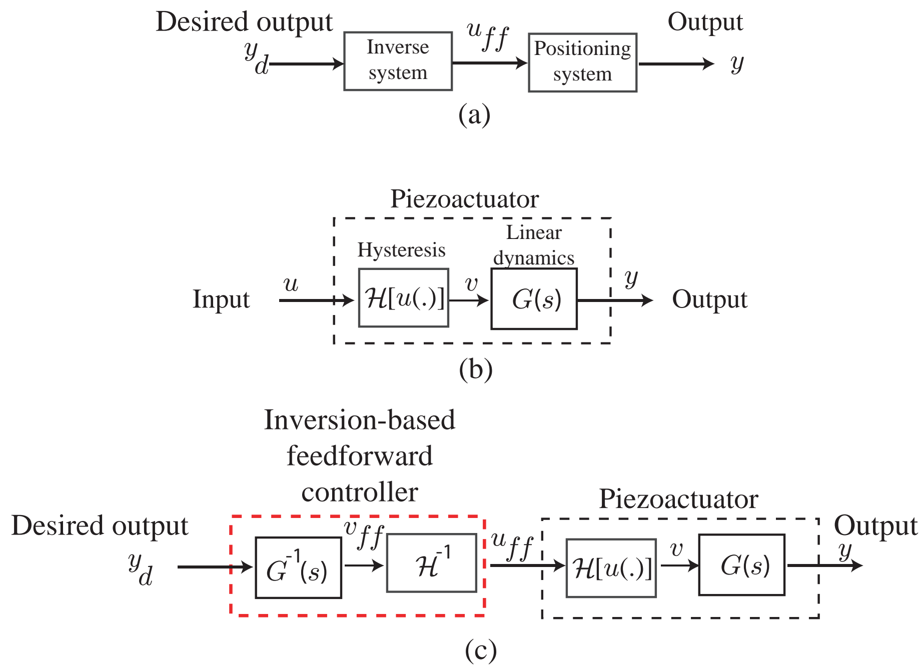


Fig. 6. Feedforward control concept: (a) block diagram of feedforward control; (b) a cascade model structure for hysteresis $\mathcal{H}[u(\cdot)]$ and vibrational dynamics and creep effects $G(s)$ in piezo-based nanopositioning systems; and (c) an inversion-based feedforward approach to compensate for dynamic and hysteresis effects.

case, the feedforward control input $u_{ff}(t)$, which accounts for both the dynamic and hysteresis effects, is obtained by passing the desired output trajectory $y_d(t)$ through the inverse models in reverse order as illustrated in Figure 6(c). This process is performed offline, followed by applying the feedforward input to the nanopositioning system. First, the dynamic inverse produces an output $v_{ff}(t)$. The output from this first stage then becomes the input to the inverse-Preisach model, which produces the final feedforward input $u_{ff}(t)$ for hysteresis and dynamics compensation.

For improved precision, an iterative-based approach, commonly known as iterative learning control (ILC) [30], can be applied to compute the feedforward input [22]. The iterative technique avoids the need to model and invert the dynamics and nonlinearities of a positioning system for feedforward control, provided that iterations can be used. Some immediate advantages is minimal system information is needed for good tracking, and if an inverse model of the system dynamics is available, it can be incorporated into the update law to dramatically improve the rate of convergence. A block diagram of the control scheme is shown in Figure 7, where $y_d$ is the desired output, and $u_k$ and $y_k$ are the input and output at the $k^{\text{th}}$ trial, respectively. The task is to design a recursive algorithm that generates an input for the next step, *i.e.*, $u_{k+1}$, such that the performance of the system is better than the previous step.

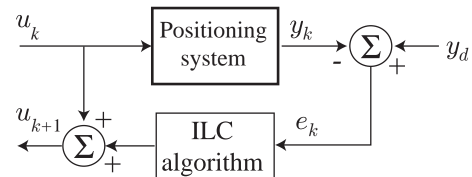


Fig. 7. Block diagram of iterative feedforward control. The iteration number is denoted by $k$.

The feedforward approach has been applied to control the motion of a piezo-based nanopositioner in an atomic force microscope (AFM) [31], [32]. Figure 8 shows AFM images that compare before and after feedforward control is applied. The hysteresis effect causes the parallel features to appear curved as shown in Figure 8(a). However, by modeling the hysteresis behavior and inverting the model for feedforward control, the resulting AFM image [Figure 8(b)] shows the true surface topology, where the distortion effect is compensated for by the feedforward input. Likewise, during high-speed scanning movement-induced structural vibrations are excited causing distortion in the form of ripples to appear across an AFM image as shown in Figure 8(c). These distortions are minimized by the feedforward approach as shown in Figure 8(d).

## References

[1] M. J. Brukman and D. A. Bonnell, "Probing physical properties at the nanoscale," *Physics Today*, vol. 61, no. 6, pp. 36–42, June 2008.

[2] Y. F. Dufrêne, "Towards nanomicrobiology using atomic force microscopy," *Nature Reviews Microbiology*, vol. 6, pp. 674–680, September 2008.

[3] D. Bonnell, Ed., *Scanning probe microscopy and spectroscopy. Theory, Techniques, and Applications. Second Edition.* Hoboken, NJ: Wiley-VCH, 2001.

[4] E. Meyer, H. J. Hug, and R. Bennewitz, *Scanning probe microscopy. The lab on a tip.* Heidelberg, Germany: Springer-Verlag, 2004.

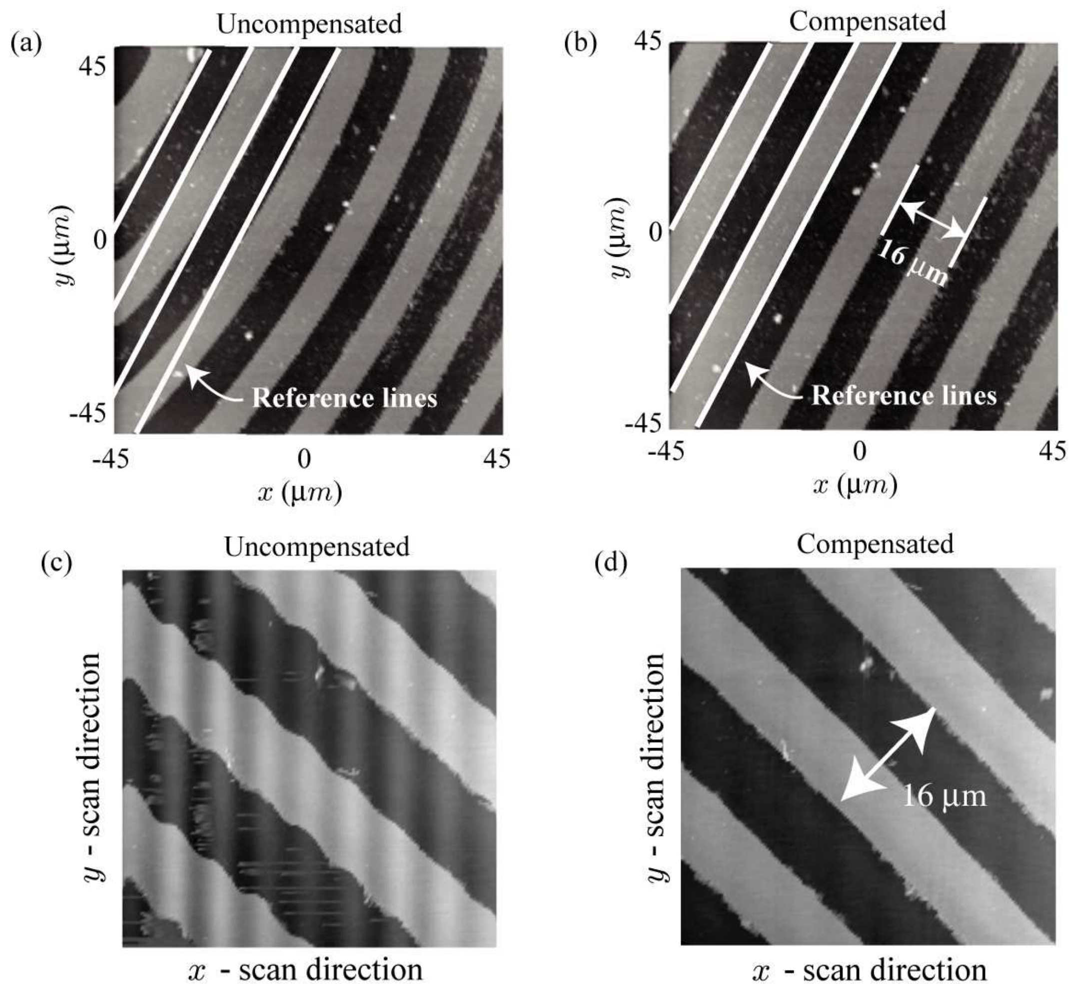


Fig. 8. AFM imaging results: (a) low-speed, without feedforward compensation; (b) low-speed, with hysteresis feedforward compensation; (c) high-speed, without feedforward compensation; (d) high-speed, with feedforward dynamics compensation.


[5] B. Bhushan, Ed., *The handbook of nanotechnology*. Springer-Verlag, 2004.

[6] D. Leonard, M. Krishnamurthy, C. M. Reaves, S. P. Denbaars, and P. M. Petroff, "Direct formation of quantum-sized dots from uniform coherent islands of ingaas on gaas surfaces," *Applied Physics Letters*, vol. 63, no. 23, pp. 3203 – 3205, 1993.

[7] G. Binnig and D. P. E. Smith, "Single-tube three-dimensional scanner for scanning tunneling microscopy," *Review of Scientific Instruments*, vol. 57, no. 8, pp. 1688–1689, August 1986.

[8] S. O. R. Moheimani, "Accurate and fast nanopositioning with piezoelectric tube scanners: Emerging trends and future challenges," *Review of Scientific Instruments*, vol. 79, no. 7, pp. 071 101(1–11), July 2008.

[9] G. E. Fantner, G. Schitter, J. H. Kindt, T. Ivanov, K. Ivanova, R. Patel, N. Holten-Andersen, J. Adams, P. J. Thurner, I. W. Rangelow, and P. K. Hansma, "Components for high speed atomic force microscopy," *Ultramicroscopy*, vol. 106, no. 2-3, pp. 881–887, June-July 2006.

[10] S. Devasia, E. Eleftheriou, and S. O. R. Moheimani, "A survey of control issues in nanopositioning," *IEEE Transactions on Control Systems Technology*, vol. 15, no. 5, pp. 802–823, September 2007.

[11] A. J. Fleming and K. K. Leang, "Charge drives for scanning probe microscope positioning stages," *Ultramicroscopy*, vol. 108, no. 12, pp. 1551–1557, November 2008.

[12] K. K. Leang and S. Devasia, "Feedback-linearized inverse feedforward for creep, hysteresis, and vibration compensation in AFM piezoactuators," *IEEE Transactions on Control Systems Technology*, vol. 15, no. 5, pp. 927–935, September 2007.

[13] A. J. Fleming, "Nanopositioning system with force feedback for high-performance tracking and vibration control," *IEEE Transactions on Mechatronics*, Accepted April 2009.

[14] D. Y. Abramovitch, S. Hoen, and R. Workman, "Semi-automatic tuning of PID gains for atomic force microscopes," in *Proc. American Control Conference*, Seattle, WA, June 2008, pp. 2684–2689.

[15] A. J. Fleming and S. O. R. Moheimani, "Sensorless vibration suppression and scan compensation for piezoelectric tube nanopositioners," *IEEE Transactions on Control Systems Technology*, vol. 14, no. 1, pp. 33–44, January 2006.

[16] S. S. Aphale, B. Bhikkaji, and S. O. R. Moheimani, "Minimizing scanning errors in piezoelectric stack-actuated nanopositioning platforms," *IEEE Transactions on Nanotechnology*, vol. 7, no. 1, pp. 79–90, January 2008.

[17] A. J. Fleming, S. S. Aphale, and S. O. R. Moheimani, "A new method for robust damping and tracking control of scanning probe microscope positioning stages," *IEEE Transactions on Nanotechnology, In Press*, 2009.

[18] A. Sebastian, A. Pantazi, S. O. R. Moheimani, H. Pozidis, and E. Eleftheriou, "A self servo writing scheme for a MEMS storage device with sub-nanometer precision," in *Proc. IFAC World Congress*, Seoul, Korea, July 2008, pp. 9241–9247.

[19] D. Croft, G. Shed, and S. Devasia, "Creep, hysteresis, and vibration compensation for piezoactuators: atomic force microscopy application," *ASME J. Dyn. Syst., Meas., and Control*, vol. 123, pp. 35–43, 2001.

[20] G. Schitter and A. Stemmer, "Identification and open-loop tracking control of a piezoelectric tube scanner for high-speed scanning-probe

microscopy," *IEEE Trans. Cont. Sys. Tech.*, vol. 12, no. 3, pp. 449 – 454, 2004.

[21] S. Devasia, "Should model-based inverse inputs be used as feedforward under plant uncertainty?" *IEEE Trans. Autom. Cont.*, vol. 47, no. 11, pp. 1865–1871, 2002.

[22] G. M. Clayton, S. Tien, K. K. Leang, Q. Zou, and S. Devasia, "A review of feedforward control approaches for nano precision positioning in high speed spm operation," *ASME J. Dyn. Syst. Meas. and Cont.*, vol. 131, p. 061101 (19 pages), 2008.

[23] K. K. Leang and S. Devasia, "Feedback-linearized inverse feedforward for creep, hysteresis, and vibration compensation in AFM piezoactuators," *IEEE Trans. Cont. Syst. Tech.*, vol. 15, no. 5, pp. 927 – 935, 2007.

[24] X. Tan and J. S. Baras, "Adaptive identification and control of hysteresis in smart materials," *IEEE Trans. Autom. Cont.*, vol. 50, no. 6, pp. 827–839, 2005.

[25] J. S. Dewey, K. K. Leang, and S. Devasia, "Experimental and theoretical results in output-trajectory redesign for flexible structures," *ASME J. Dyn. Syst., Meas., and Control*, vol. 120, no. 4, pp. 456–461, 1998.

[26] Q. Zou, "Optimal preview-based stable-inversion for output tracking of nonminimum-phase linear systems," *Automatica*, vol. In press, 2008.

[27] Q. Zou and S. Devasia, "Preview-based optimal inversion for output tracking: application to scanning tunneling microscopy," *IEEE Control Systems Technology*, vol. 12, no. 3, pp. 375–386, 2004.

[28] I. D. Mayergoyz, *Mathematical models of hysteresis*. New York: Springer-Verlag, 1991.

[29] M. Brokate and J. Sprekels, *Hysteresis and phase transitions*. New York: Springer, 1996.

[30] K. L. Moore, M. Dahleh, and S. P. Bhattacharyya, "Iterative learning control: a survey and new results," *Journal of Robotic Systems*, vol. 9, no. 5, pp. 563–594, 1992.

[31] G. M. Clayton and S. Devasia, "Image-based compensation of dynamic effects in scanning tunneling microscopes," *Nanotechnology*, vol. 16, pp. 809 – 818, 2005.

[32] K. K. Leang, Q. Zou, and S. Devasia, "Feedforward control of piezoactuators in atomic force microscope systems: inversion-based compensation for dynamics and hysteresis," *IEEE Cont. Syst. Mag.*, vol. 29, no. 1, pp. 70 – 82, 2009.

# Microrobotic tools for the measurement of small forces

S. Muntwyler, *Student Member, IEEE*, F. Beyeler, *Member, IEEE*, and B.J. Nelson, *Member, IEEE*

***Abstract*—Capacitive force and position sensing in combination with electrostatic actuation is used to design miniature tools capable of measuring forces between nano- and micronewtons to mechanically characterize microscopic samples. The functional principle of the tools as well as an introduction into the fabrication and capacitive readout are given. The calibration, being one of the most challenging parts of microforce sensing, as well as the methods to calculate the sensing uncertainty are presented.**

## I. Introduction

One of the key engineering objectives in microrobotics is the sensing of microscale forces, to provide a feedback for controlling the micromanipulation process. In other fields like mechanobiology, material science and life science a trend towards the measurement of mechanical properties of ever-smaller samples can be seen. During the past few years, the focus in e.g. plant development biology has shifted from studying the organization of the whole body or individual organs towards the behavior of smallest units of the organism, the single cell [1].

The aim of this research is to develop novel tools to provide researchers in different fields with the means to gather quantitative information on the mechanical properties of microscopic samples. An assortment of miniature force sensors capable of measuring forces in the micro- to nanonewton range have been developed and successfully used in a variety of applications. In [2, 3] the design of a single- axis capacitive force sensor and its application to study insect flight control, the mechanical characteristics of mouse embryo cells and the threshold for touch sensation in C. elegans [4] are shown. In [5] a sensor based on an optical, diffractive micrograting demonstrates the measurement of the injection forces into drosophila embryos and in [6] the use of an atomic force microscope (AFM), based on optical beam deflection, shows the measurement of molecular interaction forces. A sensor based on the trapping of a magnetic particle in a magnetic field is shown in [7] and is used to measure the force- extension curves of DNA molecules.

## II. Capacitive based tools

The focus of this research lies in the development of capacitive based microforce sensors capable of measuring

Manuscript received February 25, 2010. This work is conducted with financial support from the project "Hybrid Ultra Precision Manufacturing Process Based on Positional and Self-assembly for Complex Micro- Products (HYDROMEL)" funded by the European Commission under the 6th Framework Program (FP6).

S. Muntwyler, F. Beyeler and B.J. Nelson are with the ETH Zurich, Zurich, CH 8092 Switzerland (msimon@ethz.ch, fbey@ethz.ch, bnelson@ethz.ch).

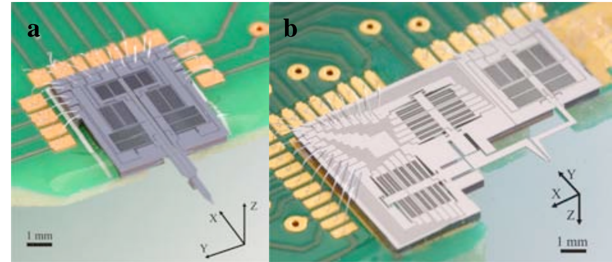


Fig. 1. a) MEMS-based capacitive three-axis microforce sensor. b) Monolithic integrated two-axis micro-tensile tester

forces in the range from nano- to millinewtion. Capacitive force sensors offer advantages, such as a high signal-to-noise ratio the ability to measure static as well as dynamic forces with frequencies up to a few kHz and virtually no sensitivity to temperature, humidity or illumination conditions. Capacitive one, two and three axis forces sensors (figure 1a) have been developed. These sensors consist of a movable body suspended by flexures within an outer frame. A force applied to the probe, attached to the movable body, results in a relative motion of the body and the frame, which can be measured by attached capacitive electrodes as a change of capacitance. By allowing the sensor to move in multiple directions and by using several of these capacitive displacement sensors, forces in multiple axes can be measured.

By combining the force sensors with electrostatic actuators complete measurement systems can be realized, such as a two axis monolithically integrated micro-tensile tester shown in figure 1b. The sample e.g. a cell is measured between the tips of the two end-effectors. The right end-effecter arm is connected to a two-axis microforce sensor allowing it to simultaneously measure forces and the position of the end-effecter in x- and y-direction. The left arm is connected to a platform suspended by flexures within two orthogonally attached actuators. Both actuators can move along one axis (x or y) and offer position feedback, therefore the platform can be actuated in two axes and assuming a rigid body, the position of the end-effecter can be measured in x- and y-directions.

## III. Microfabrication

The capacitive based tools presented, are fabricated using a MEMS (Micro-Electro-Mechanical System) bulk silicon micro-fabrication process. For in plane electrostatic actuation and capacitive sensing a silicon-on-Insulator (SOI) process described in [8] is used. It involves the etching of the thick handle layer (400 μm thick) as well as the buried oxide (BOX) around the outer frame of the sensor and

subsequently etching of the active elements like the flexures and the capacitors as well as the body of the devices into the 50 µm thick device layer. In the case of the three-axis force sensor also out of plane motions need to be detected. Therefore instead of only a single device layer, a double SOI wafer is used with two device layers (each 25 µm thick). By measuring the capacitance between the top device layer of the fixed electrode and the lower device layer of the movable electrode an out of plane motion can be detected [9].

## IV. Capacitive Readout

The main drawback of capacitive position or force sensing is the non-linear relationship between the change of capacitance and the electrode distance. This is overcome by differentially measuring two capacitive changes in opposite directions. A commercial capacitance-to-voltage converter IC (CVC1.1, GEMAC) is used to interface each capacitor pair on the sensor. More details about capacitive sensing can be found in [10].

## V. Sensor Calibration

Precise calibration of multi-axis MEMS force sensors is difficult for several reasons, including the need to apply known force vectors at precise positions and orientations which risk damaging the small and fragile microdevices [11].

The most commonly used microforce sensor, the AFM, has led to the development of a large number of methods to calibrate forces in the micro- and nanonewton range [12]. However, the accuracy of these methods is unknown since none of them are traceable to the Systeme International (SI) d'unite´s. The unit force is derived from the definition of Newton using a combination of base SI units (kg, m and s) [13].

The capacitive sensors measure a change of the position or the force as a change of the sensor output voltage. But the exact numerical relationship is not known a priory. A common approach to this problem is to model this relationship by e.g. an FEM model. But due to imperfections in the microfabrication process, e.g. over etching of the flexure elements, the results will be inaccurate and more importantly the measurement cannot be traced back to the SI units.

The position and force sensors are calibrated by comparing them with a reference standard. For the measurement of the displacements a microscope with attached camera is used. The system is pre-calibrated using a standard optical target (USAF 1951, Edmund optics). For the calibration of the force sensors, a custom build reference force sensor is used, which is pre-calibrated using weights with a known mass, pre-calibrated using a semi-micro-balance (XS205DU, Mettler Toledo) for which the uncertainty is known.

Using a micromanipulator the reference force sensor is pushed against the microforce sensor. By comparing the sensors output voltage and the applied force, the calibration coefficients of the sensor can be found.

## VI. Uncertainty Analysis

The result of a measurement is only an approximation of the value of the measurand and, thus, is complete only when accompanied by a statement of the uncertainty of that estimate [14]. The measurement uncertainty is a parameter associated with the results of a measurement that characterizes the dispersions of the values that could reasonably be attributed to the measurand [15].

Therefore, besides the calibration coefficients, the most important characteristics of the sensors are measured and their influence onto the measurement uncertainty calculated.

The Joint Committee for Guides in Metrology (JCGM) of the Bureau Interanational des Poids et Mesures (BIPM) has a working group with responsibility for the expression of uncertainty in measurement. They have published the ISO Guide to the Expression of Uncertainties in Measurements (GUM) [14], which has become the internationally accepted master document for the evaluation and combination of these uncertainties. In the GUM a deterministic method based on the law of propagation of uncertainties and on the characterization of the measured input quantities be either normal or t-distribution, allowing the calculation of coverage intervals for the output quantities. To deal with cases, which cannot reasonably be approximated by Taylor series expansions and involve other PDF e.g. rectangular, a supplement 1 has been added to the GUM describing the Monte Carlo method. This method evaluates the propagation of distribution by performing random sampling from the input probability distributions. And in the latest supplement these methods have been extended two multivariate problems with any number of output quantities.

## VII. Conclusion

Capacitive sensing is used to measure small force and position changes. In combination with electrostatic actuators entire measurement systems can be realized capable of mechanically characterizing microscopic samples. The sensor calibration and the calculation of its uncertainties remain one of the most challenging problems in microforce sensing,

Increasing effort is being made in multiple national measurement institutes (NMI) to create an SI traceable reference standard for the calibration of small forces. An overview of the different approaches can be found in [13].

## References


[1] M. Hulskamp, "Plant trichomes: A model for cell differentiation," Nature Reviews Molecular Cell Biology, vol. 5, pp. 471-480, Jun 2004.

[2] Y. Sun and B. J. Nelson, "MEMS capacitive force sensors for cellular and flight biomechanics," Biomedical Materials, vol. 2, pp. S16-S22, Mar 2007.

[3] C. F. Graetzel, S. N. Fry, F. Beyeler, Y. Sun and B. J. Nelsons, "Real-time microforce sensors and high speed vision system for insect flight control analysis," Experimental Robotics, vol. 39, pp. 451-460

[4] J. C. Doll, S. Muntwyler, F. Beyeler, S. Geffeney, M. B. Goodman, B. J. Nelson, B. L. Pruitt, "Measuring Thresholds for Touch Sensation in C. Elegans", Proc. in the 5th International Conference on Microtechnologies in Medicine and Biology (MMB), Québec, Canada, April 2009.

[5] X. J. Zhang, et al., "Integrated optical diffractive micrograting-based injection force sensor," Boston Transducers'03: Digest of Technical Papers, Vols 1 and 2, pp. 1051-1054

[6] T. Hugel and M. Seitz, "The study of molecular interactions by AFM force spectroscopy," Macromolecular Rapid Communications, vol. 22, pp. 989-1016, Sep 18 2001.

[7] C. Gosse and V. Croquette, "Magnetic tweezers: Micromanipulation and force measurement at the molecular level," Biophysical Journal, vol. 82, pp. 3314-3329, Jun 2002.

[8] F. Beyeler, et al., "Design and calibration of a MEMS sensor for measuring the force and torque acting on a magnetic microrobot," Journal of Micromechanics and Microengineering, vol. 18, pp. -, Feb 2008

[9] S. Muntwyler, F. Beyeler and B. J. Nelson, "Three-axis micro-force sensor with sub-micro-Newton measurement uncertainty and tunable force range," Journal of Micromechanics and Microengineering, p. 025011, 2010.

[10] Y. Sun, S. N. Fry, D. P. Potasek, D. J. Bell and B. J. Nelson, "Characterizing fruit fly flight behavior using a microforce sensor with a new comb-drive configuration," Journal of Microelectromechanical Systems, vol. 14, pp. 4-11, Feb 2005.

[11] K. Kim, Y. Sun, R. M. Voyles and B. J. Nelson, "Calibration of multi-axis MEMS force sensors using the shape-from-motion method," Ieee Sensors Journal, vol. 7, pp. 344-351, Mar-Apr 2007.

[12] N. A. Burnham, et al., "Comparison of calibration methods for atomic-force microscopy cantilevers," Nanotechnology, vol. 14, pp. 1-6, Jan 2003.

[13] J. R. Pratt, J. A. Kramar, D. B. Newell and D. T. Smith, "Review of SI traceable force metrology for instrumented indentation and atomic force microscopy," Measurement Science & Technology, vol. 16, pp. 2129-2137, Nov 2005.

[14] ISO, "Guide to the expression of uncertainty in measurement," Geneva, Switzerland, 1995.

[15] P. M. Clifford, "The International Vocabulary of Basic and General Terms in Metrology," Ptb-Mitteilungen, vol. 94, pp. 419-423, 1984.

# In situ Characterizations of Thin-film Nanostructures with Large-range Direct Force Sensing

Gilgueng Hwang and Stéphane Régnier, *Member, IEEE*

***Abstract*— Recently, many different types of thin-film nanostructures such as semiconductor nanofilms, single atomic layer carbon nanofilms (graphene) have been synthesized toward their nanoelectronics and nanoelectromechanical systems (NEMS) applications. However the precise electrical and mechanical properties of these structures are still being required. We introduce in situ characterizations with direct force sensing in large range but high resolution toward the NEMS based on thin-film nanostructures.**

***Index Terms*— Nanomanipulation, force sensing, helical nanobelts, tuning forks**

## I. Introduction

Micro/nanomanipulation and assembly are important technologies toward the development of micro-nanoelectromechanical systems (MEMS/NEMS) [1-3]. However these manipulations are currently being performed by human operators manually which makes the task very stressful and time-consuming. It is mainly because of the lack of proper sensing tools to measure different physics in micro/nano scale. Currently available sensors cannot measure such different physical transitions because of their limited sensing resolution and range (Figure 1).

For an automated micro/nanomanipulation, it is necessary to have both visual and force feedback. In-situ scanning electron microscope (SEM) nanomanipulation was proposed to combine good enough visual feedback but the force sensing is still in their infancy. Therefore we report our work on the high resolution, wide range force sensing with helical nanobelts and tuning forks that can be utilized in the in-situ SEM nanomanipulation system.

The developed force sensing mechanisms can also be utilized to characterize the mechanical properties of ultra-flexible nanostructures. Mechanical property characterizations of ultra-flexible three-dimensional nanostructures are important during the development of NEMS. It also requires ultra-high precision and wide range force calibration.

For even much higher resolution of sensing, optical tweezers [4], magnetic bead [5], and atomic force microscopy (AFM) [6] have been mostly studied, and AFM among them is the mostly used. However these methods are limited in large displacement measurement and principal difficulty to measure 3-D forces and suffer from several limitations such as their limited force and displacement ranges. Considering the force resolution, optical method can easily reach piconewtons to the contrary of the other methods which are in the upper range of nanonewtons [7]. Furthermore cantilevers need strong calibration and are difficult to be used as a sensor or actuator for several dimensions (the cantilever's torsion is difficult to characterize). Optical tweezers are useful for a large variety of object to characterize, however they are strictly limited in the piconewton range of the forces to measure. For studies that require larger forces, atomic force microscope cantilevers are more suitable choices because they are stronger (less compliant) than optical tweezers. Finally, their potential integration with experimental setup is challenging and expensive because of necessary external laser optics, especially in vacuum.

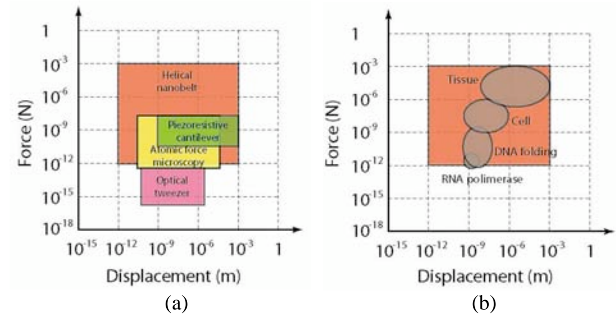


(a) (b)

Fig. 1. Large displacement/force sensing measurement tools (a) and applications (b).

The studied whole systems are limited in their force range or in their displacement range (Figure 1). To build a sensor which is able to measure piconewton as well as millinewton and capable of picometer displacements as well as millimeter displacement still remains a challenging research area. The newly proposed sensor would then be useful in a wide variety of objects to characterize such as nanowires, tissues, viruses, bacteria, living cells, colloidal gold, and even DNA. The further advantage consists in its simple and straightforward integration that will lead to the conception of complex MEMS (nano-translators with high displacement range, nano-sensors with high force range) for future complex bio- or non-organic applications.

The aim of this workshop is to introduce our recent works in development of large range force sensing tools

G. Hwang and S. Régnier are with the Institut des Systèmes Intelligents et de la Robotique, Université Pierre et Marie Curie, 4 Place Jussieu, 75005 Paris, France (phone: +33-1-44-27-6370; fax: +33-1-44-27-5145; e-mail: hwang@isir.upmc.fr).

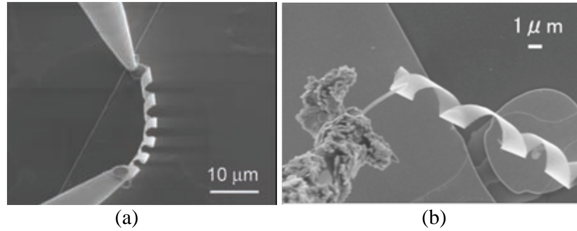


(a) (b)

Fig. 2. Metal connector attached 3-D helical nanobelts and their electromechanical property characterization with two metal probes. (a) The piezoresistivity was characterized in the longitudinal tensile elongations. (b) mechanical property of silicon nanowire is characterized by helical nanobelts

(micronewton range with the resolution of hundreds of piconewton) for in situ property characterizations of ultra flexible nanostructures. For this purpose, the sensors should be integrated to electron microscopes. Thus the sensors should also be vacuum and electron beam compatible. For this aim, we are currently developing two different types of force sensors. In this workshop, the first part will describe the 3-D piezoresistive helical nanobelt (HNB) force sensors and their applications. Then the tuning fork based force sensors will be shown. Using these tools, we therefore can study electromechanical properties of ultra-flexible nanostructures by in-situ scanning electron microscope (SEM) nanomanipulation with direct force characterization by incorporating nanomanipulators.

## II. Large Range Force Sensing Tools

### A. *Piezoresistive Helical Nanobelts as Force Sensors*

HNBs with metal pads attached on both sides were fabricated using conventional microfabrication techniques (Figure 2a) [8]. With the metal connectors, good electrical contact can be achieved. Besides the electromechanical characterization, such connectors also allow for the integration of these structures into more complex assemblies. Nanomanipulation inside an SEM was used for their electromechanical property characterization. The experimental results showed that the structures exhibit a unusually high piezoresistive response. Moreover, electrostatic actuation was used to excite the structures at their resonance frequency and investigate their resistance to fatigue. With their low stiffness, high strain capability, and good fatigue resistance, the HNBs can be used as high-resolution and large-range force sensors. By variation of design parameters, such as the number of turns, thickness, diameter, or pitch, a HNB with the required stiffness can be designed through simulation. The fabrication process is suitable for further miniaturization. Nanometer scale diameter and wire width can be achieved through changes in the later design and by using electron-beam lithography, respectively.

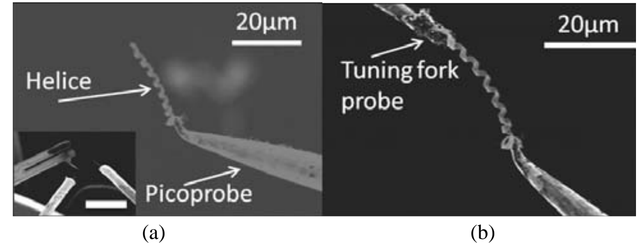


(a) (b)

Fig. 3. Tuning fork force calibration using HNB: (a) HNB picked with probe of manipulator (inset figure depicts the two probes of manipulators and tuning fork for manipulation and calibration of HNB), (b) the picked HNB was attached to the probe of tuning fork).

### B. *Tuning Fork Force Sensor*

As another force sensing tool, tuning fork was utilized to function in dynamic force measurement applications. The wide range (16.6pN - 500 nN) force sensor based on tuning fork and FM-AFM method was developed. Attaching a high aspect ratio probe tip onto tuning fork enabled amplification to the amount of stress applied to the tuning fork body. The measured frequency shift of tuning fork was calibrated with as-calibrated cantilever in the nano-newton range force and HNBs with the stiffness estimation from the model for the sub-nanonewton range (Figure 3). The demonstrated force sensors are easily integrated to SEM thus the demonstrated technology have strong potential in nanomanipulations of various nanostructures.

### C. *Potential Applications*

The static nanomechanical characterization of ultra-thin film nanostructures is promising application of the proposed HNB force sensors. Since the device is based on smart sensing with simple current monitoring to measure the force, any complicated external read-out devices are not required. We have been applied these sensors to characterize the mechanical properties of silicon nanowires and graphene with even smaller dimensions (Figure 2b). Visual tracking of the deformation is also promising to measure the force using HNBs in case of wet applications such as biological manipulation.

Furthermore, tuning fork force sensors can be applied to reveal mechanical properties of the dynamic systems such as resonators based on thin membrane nanostructures. By incorporating with cryogenic or biological manipulation setup, it can also be utilized to measure the dynamically varying biological nanostructures.

## Acknowledgment

We thank the clean room staffs of LPN/CNRS for technical support. The authors thank the French Atomic Energy Commission (CEA) Fontenay aux Roses for the SEM and facilities, and the University of Tokyo for allowing us to use the two Kleindiek manipulators with their respective controllers. We thank Guy Blaise for his SEM expertness at INSTN of CEA Saclay. We also thank Jacques Cousty, Christophe Lubin and Laurent Pham Van

for the fruitful discussions. This work has been supported by the French National Project NANOROL ANR-07-ROBO-0003.

## References

[1] J. Abbott, Z. Nagy, F. Beyeler, and B. Nelson, “Robotics in the small, part i : Microbotics,” Robotics & Automation Magazine, IEEE, vol. 14, no. 2, pp. 92–103, 2007.

[2] L. Dong and B. Nelson, “Tutorial - robotics in the small part II: nanorobotics,” Robotics & Automation Magazine, IEEE, vol. 14, no. 3, pp. 111–121, 2007.

[3] B. Nelson, L. Dong, A. Subramanian, and D. Bell, “Hybrid nanorobotic approaches to NEMS,” in Robotics Research, pp. 163–174, 2007.

[4] K. Nagato, Y. Kojima, K. Kasuya, H. Moritani, T. Hamaguchi, and M. Nakao, “Local synthesis of tungsten oxide nanowires by current heating of designed micropatterned wires,” Applied Physics Express, vol. 1, pp. 014005, 2008.

[5] K. S. Novoselov, A. K. Geim, S. V. Morozov, D. Jiang, Y. Zhang, S. V. Dubonos, I. V. Grigorieva, and A. A. Firsov, “Electric field effect in atomically thin carbon films,” Science, vol. 306, no. 5696, pp. 666–669, Oct. 2004.

[6] Y. Sun, B. J. Nelson, and M. A. Greminger, “Investigating protein structure change in the zona pellucida with a microrobotic system,” The International Journal of Robotics Research, vol. 24, no. 2-3, pp. 211–218, Feb. 2005.

[7] Y. Sun and B. J. Nelson, “MEMS for cellular force measurements and molecular detection,” Journal of Information Acquisition, vol. 1, no. 1, p. 23–32, 2004.

[8] G. Hwang, H. Hashimoto, D. J. Bell, L. X. Dong, B. J. Nelson, S. Schön, "Piezoresistive InGaAs/GaAs Nanosprings with Metal Connectors", Nano Letters, Vol. 9, No. 2, pp. 554-561, February 2009.

# *In-Situ* Mechanical Characterization of Mouse Oocytes Using a Cell Holding Device

Xinyu Liu[1], Roxanne Fernandes[2], Andrea Jurisicova[2], Robert F. Capser[2], and Yu Sun[1]

Biological cells have several mechanical elements, such as the membrane and cytoskeleton (actin and intermediate filaments; microtubules) that define cellular mechanical properties, shape, and functions. Quantification of cell mechanical properties is not only important for understanding cellular structure and function but also useful for assessing cell quality. This abstract presents our recent work on characterizing mechanical properties of healthy mouse oocytes and those with compromised development competence during microrobotic cell injection (i.e., *in situ*).

Cellular force measurement is a must for cell mechanical characterization. Macro-scale force sensors can be used to measure forces on zebrafish embryos (~1.2 mm) with a low force resolution (tens of micronewton), but are now applicable for characterizing smaller cells (e.g., ~100 µm mouse oocyte/embryo). Although silicon-based MEMS force sensors provide nanonewton force measurement resolution [1, 2], they do not allow for an easy integration of the fragile MEMS devices and the micropipette. Previously reported PDMS post arrays [3, 4] can measure contraction forces of adherent cells; however, they do not permit mechanical characterization of suspended cells, such as mouse oocytes.

This abstract presents a PDMS cell holding device and its application to *in situ* mechanical characterization of mouse oocytes. The device is used together with a visual tracking algorithm for resolving nanonewton-level cellular forces during microrobotic injection of mouse oocytes. We previously developed a large-sized PDMS device and applied it to measuring forces on zebrafish embryos (~1.2 mm) with a micronewton force resolution [5]. The study presented here focuses on miniaturizing the devices for smaller mouse oocytes (~100 µm), enhancing the force resolution to nanonewton, and using *in situ* obtained data to distinguish defective oocytes from healthy ones for better selecting oocytes in genetics and reproductive biology.

Fig. 1 illustrates the working principle of the device. While the micropipette injects a mouse oocyte inside a device cavity, applied forces are transmitted to low-stiffness supporting posts. In real time, a sub-pixel computer vision tracking algorithm measures post deflections that are fitted into an analytical mechanics model to calculate the force exerted on the oocyte. Fig. 2 shows a SEM picture of the device, fabricated using standard soft lithography. The supporting posts are 45µm high and 12µm in diameter. Young's modulus of the posts was calibrated via nanoindentation to be 524.7±22.1 kPa (n=5). A computer vision algorithm was developed to track post deflections at 30 Hz with a resolution of 0.5 pixel. The force measurement resolution was 2 nN. Fig. 3 shows an indented mouse oocyte and deflected posts that are tracked and labeled by circles. An analytical mechanics model (Fig. 4) was developed to map post deflections into cellular forces.

The device was used within a microrobotic cell injection system. Oocytes obtained from aged mice often exhibit cellular defects, such as meiotic spindle defects causing chromosomal abnormalities and mitochondrial dysfunction. The purpose was to determine whether mechanical characterization can provide useful cues for distinguishing healthy and defective oocytes. In experiments, 20 oocytes from young ICR mice and 20 oocytes from old ICR mice were characterized during microinjection. Fig. 5 shows the collected force-deformation curves. Most of the curves of young and old oocytes separate themselves distinctly with a slight overlap of a few curves. Stiffness of the young and old oocytes (Table 1) was significantly different ($p<0.001$).

SEM analysis of the zona pellucida (ZP - the outer membrane), showed that 80% of old oocytes have different ZP surface morphology (Fig. 6(b)) than young oocytes (Fig. 6(a)). TEM imaging of ZP glycoprotein organization (Fig. 6(c)(d)) indicated that old oocytes have a significantly lower ($p<0.001$) glycoprotein density (Table 1) than young oocytes, which translates into lower ZP stiffness in old oocytes. Fluorescence analysis of oocyte F-actin (Fig. 7) demonstrated that old oocytes have decreased F-actin ($p<0.001$) with subcortical region particularly lacking this cytoskeletal protein. Thus, structural differences of aged oocytes caused by altered distributions of ZP and F-actin likely contribute to the measured mechanical differences. These results demonstrate that technique can be useful for distinguishing healthy and defective oocytes during cell injection, without requiring a separate characterization process.

[1] Xinyu Liu and Yu Sun are with the Advanced Micro and Nanosystems Laboratory, University of Toronto, 5 King's College Road, Toronto, ON, Canada, M5S 3G8. sun@mie.utoronto.ca.

[2] Roxanne Fernandes, Andrea Jurisicova, and Robert F. Casper are with Samuel Lunenfeld Research Institute, Toronto Mount Sinai Hospital.

## References

[1] Y. Sun, K. T. Wan, K. P. Roberts *et al.*, "Mechanical property characterization of mouse zona pellucida," *IEEE Trans. Nanobiosci.*, vol. 2, no. 4, pp. 279-286, 2003.

[2] S. Y. Yang, and M. T. A. Saif, "MEMS based force sensors for the study of indentation response of single living cells," *Sens. Actuator. A - Phys.*, vol. 135, no. 1, pp. 16-22, 2007.

[3] J. L. Tan, J. Tien, D. M. Pirone *et al.*, "Cells lying on a bed of microneedles: An approach to isolate mechanical force," *Proc. Nat. Acad. Sci. USA,* vol. 100, no. 4, pp. 1484-1489, 2003.

[4] Y. Zhao, and X. Zhang, "Cellular mechanics study in cardiac myocytes using PDMS pillars array,"*Sens. Actuator. A - Phys.,* vol. 125, no. 2, pp. 398-404, 2006.

[5] X. Y. Liu, Y. Sun, W. H. Wang *et al.*, "Vision-based cellular force measurement using an elastic microfabricated device," *J. Micromech. Microeng.,* vol. 17, no. 7, pp. 1281-1288, 2007.

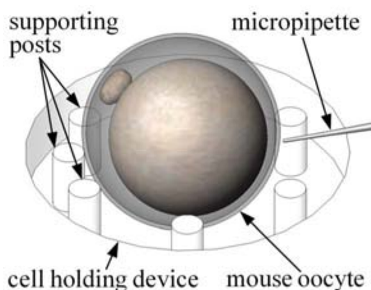


Fig. 1. Cellular force measurement using low-stiffness elastic posts during microinjection.

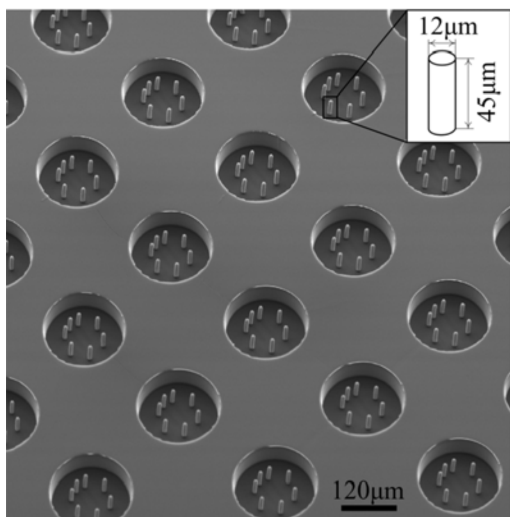


Fig. 2. SEM image of the PDMS cell holding devices.

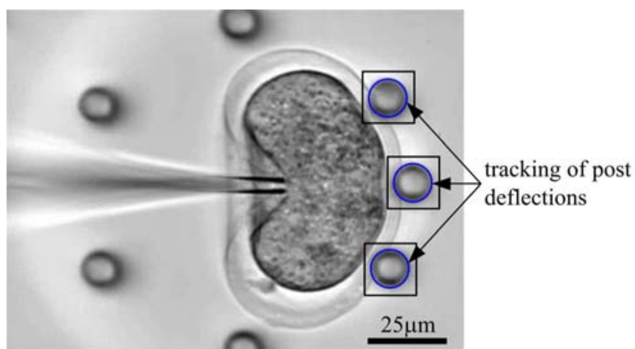


Fig. 3. Indentation forces deform the mouse oocytes and deflect three supporting posts. Blue circles label the tracking results of post deflections.

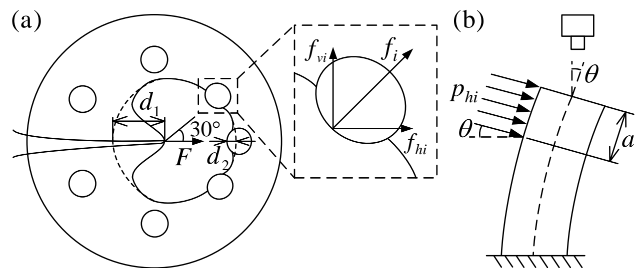


Fig. 4. Injection force analysis. (a) Force balance on the cell under indentation. (b) Post deflection model.

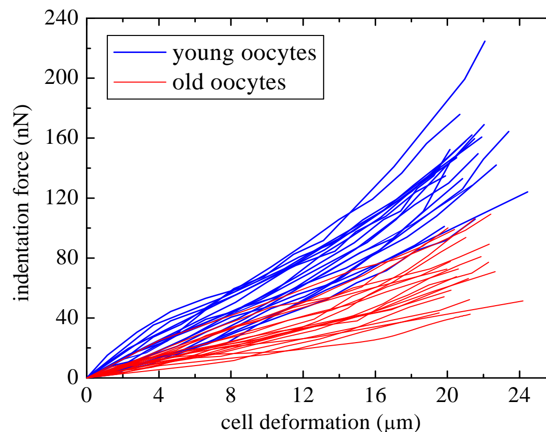


Fig. 5. Force-deformation curves of young and old oocytes.

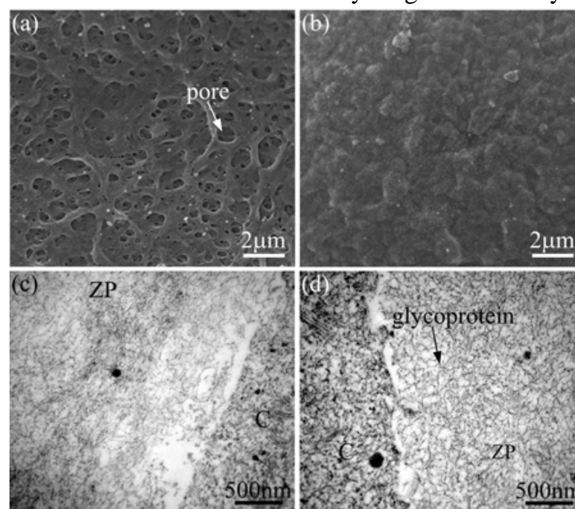


Fig. 6. (a)(b) SEM images of (a) 'spongy' ZP surfaces of young oocytes and (b) compact and rough ZP surfaces of old oocytes. (c)(d) TEM images of ZP glycoproteins of (c) young oocytes and (d) old oocytes. C: cytoplasm.

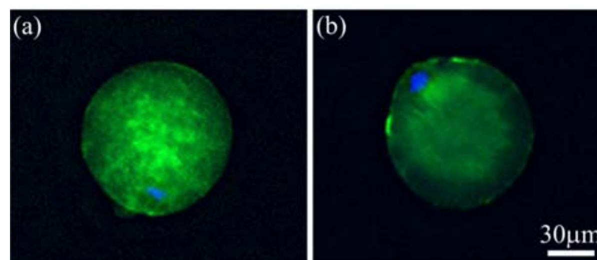


Fig. 7. F-actin staining images of (a) young oocytes and (b) old oocytes. Old oocytes have significantly less ($p<0.001$) F-actin than young oocytes. Green: F-actin. Blue: nucleus.

Table 1. Experimental data of oocyte stiffness, relative density of ZP glycoproteins, and F-actin contents.

| | Young oocytes | Old oocytes |
|---|---|---|
| Stiffness (nN/μm) | 6.4±1.3 (n=20) | 3.3±0.9 (n=20) |
| Relative density of ZP glycoproteins (%) | 44.9±1.6 (n=8) | 37.9±0.8 (n=8) |
| F-actin contents (fluorescence unit $\times 10^6$) | 1.9±0.52 (n=12) | 1.07±0.42 (n=10) |

# Observer-based estimation of weak forces in a nanosystem measurement device

A. Voda and G. Besançon

*Abstract*— **This paper presents an observer-based approach for weak force measurement via AFM experiments: the idea is to directly reconstruct the force to be measured, from the cantilever deflection actually measured by an optical device and some appropriate observer design. This design classically relies on a dynamic model, which is here beforehand identified. The proposed method is shown to be fairly efficient via experimental illustrative results.**

*Index Terms*— **State observer, model identification, force measurement, AFM, experimental set-up.**

## I. INTRODUCTION

Atomic Force Microscopy (AFM) is a powerful measurement tool to detect weak forces at a very low scale. Since the first apparatus designed by G. Binnig and H. Rohrer in 1986 ([Binnig et al.(1986)Binnig, Quate, and Gerber]), numerous operation modes have been developed to image a sample and to extract various local physical properties. However, the heart of the device remains roughly the same: it consists of a microlever bearing a tip at its end, on which a force exerted by a sample is applied. Additional excitation forces can be implemented, through a bimorph for instance, to run specific measurement (dynamic AFM). Microlever motion, generated by external force, is acquired through various techniques (spot laser deflection, interferometer, piezoresistive microlever, and so on) and determines the raw signal of an experiment. It is connected to the force within microlever mechanical response: as a result, force signal can strongly differ from it. *The method proposed in this paper aims at addressing the issue of force reconstruction via observer strategy.*
Sample analysis in biology, chemistry and materials physics require more powerful tools to increase amounts of data to be processed. For instance, biological processes, such as DNA replication, protein synthesis or drug interaction, are largely governed by intermolecular forces. As AFM has the ability to measure weak forces in the sub-nanonewton range, this makes it possible to quantify the molecular interaction in biological systems such as a variety of important ligand-receptor interactions. In addition to measuring binding forces, AFM can also probe the micromechanical properties of biological samples, since it can observe the elasticity and the viscosity of samples like live cells and membranes. In this context, force estimation requires efficient methods to improve sample analysis. Numerous trade-offs have to be done when selecting microlever model, scanning method and its relative parameters. Force reconstruction may improve analysis ability of AFM device by reducing scanning time, and it can offer a more comprehensive control of the system. Such a strategy can further extend to other relative fields, from manipulation of nano-objects to inertial sensors, as they arise in nanosciences.

¿From a system viewpoint, the problem of force measurement can be considered as a problem of internal information reconstruction, or, in a state-space formalism, a problem of *observation* ([Kwakernaak and Sivan(1972)]).
The present paper thus recasts the problem of force measurement in that spirit, focusing on a very simple formulation for the sake of illustration. The purpose is then to present and use some appropriate experimental set-up with the purpose of experimentally illustrating and validating the implementation and performances of the proposed methodology.

The considered AFM set-up and measurement problem is thus first explained in section II. The proposed observer approach is then described in section III. Some experimental validating device and corresponding observer-based force reconstruction results are finally presented in IV, while some conclusions end the paper in section V.

## II. CONSIDERED AFM MODEL AND FORCE MEASUREMENT PROBLEM

The basic AFM principle can be understood from figure 1 hereafter: it is basically made of a cantilever bearing a tip, which is approached to a sample. Both the cantilever and the sample can be appropriately positioned via a couple of drivers. The deflection of the lever end, denoted by z, is generated by forces appearing between the tip and the sample. Numerous operation modes have been implemented to run sample analysis: most of them consist in keeping the mechanical state of the lever constant by appropriately changing tip sample distance while scanning sample surface. This operation makes it possible to get surface topology. These mechanical states depend on tip sample distance and can be the deflection in case of contact AFM, amplitude deflection or resonance frequency in case of dynamic mode (Tapping, AM/FM AFM) (see [Albrecht et al.(1991)Albrecht, Grütter, Horne, and Rugar], [Giessibl(2003)], [García and Pérez(2002)]).

This work was not supported by any organization

A. Voda and G. Besançon are with Control Systems Department[1] GIPSA-lab, Grenoble University, UMR 5216, BP 46 38402 Saint-Martin d'Hères, France alina.voda@gipsa-lab.grenoble-inp.fr

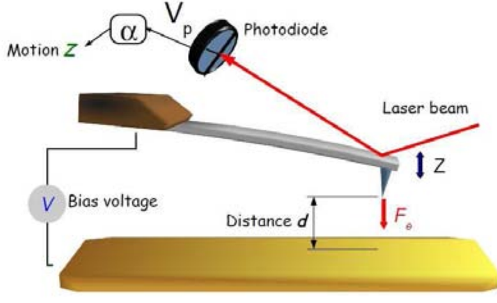


Fig. 1. **Considered AFM setup. The microlever (Mikromash CSC37 Ti-Pt lever B) has a conductive coating on both side. It is located at a distance $d \approx 1\ \mu m$ from the gold sample surface. A bias voltage is put on the tip with respect to the sample, thus generating an electrostatic force $F_e$ on it. Microlever motion $X$ is picked up through a laser beam deflection system.**

In addition, various physical properties can be drawn from the interaction of the tip with the sample to be analyzed: electrostatic, magnetic, thermal or mechanical properties. Lever motion resulting from the interaction of the tip with the sample provides the signal to be processed by the AFM operation mode. In this context, force estimation is mostly not a prerequisite. The problem we consider here is that of measuring the force between the sample and the tip via the measurement of deflection z.

First, a description of the system requires mechanical response modeling of the lever undergoing a force $F$ at its end. Then various noise sources are added to account for signals experimentally acquired. Starting from the Euler-Bernouilli theory of Beam (e.g. as in [Cleland(2004)], [Clough and Penzien(1993)]), it appears that the dynamical behaviour of the whole lever can be represented by a set of harmonic vibration modes having different resonance frequencies. Reducing the lever motion to the first flexural vibration mode proved to be a convenient and relevant approximation, when working at low frequency, below and around the first resonance frequency. The discrepancy resulting from not taking into account upper modes is estimated to be lower than a few percent, as it will be shown in the system identification section. As a result, we get a model of the following classical form:

$$m\ddot{z}(t) + f\dot{z}(t) + kz(t) = F(t, d) \tag{1}$$

where $m$,$k$, $f$ respectively stand for the effective mass of the cantilever and the first mode stiffness and friction coefficients, while $F$ is the force between the tip and the sample. The observation method which is advocated here can actually include several modes in estimating the lever motion: this capability has to be used when working on higher frequency signal. However the present paper aims at presenting the method principle and is therefore based on a simpler model.

In addition to the classical representation (1), the coupling of the device with the environment depicted as a thermal bath at temperature $T = 300$ K results in a thermo-mechanical force noise further affecting the dynamics, denoted by $f_n$. It is related to the stochastic part of the Langevin force, which also includes the damping force $-f\dot{z}$ acting on the system. Statistic physics requires force noise density $S_f$ to be related to damping coefficient $f$, so that the elastic energy or kinetic energy of the first mode are equal to $(k_bT)/2$ (with $k_b$ the Boltzmann constant $= 1.3806 \times 10^{-23} J.K^{-1}$). As a result the force noise density, which is assumed to be white, can be expressed as $S_{f_n} = 4k_bTf$. Then the mechanical response of the lever acts as a resonant filter on the thermal mechanical force noise. In this context, the lever motion can be broken down into component $z$ generated by force $F$ and component $z_n$ generated by force noise $f_n$, which corresponds to a stochastic motion with spectral density $S_{z_n}$:

$$S_{z_n} = |H(\omega)|^2 S_{f_n} \tag{2}$$

where $|H(w)|$ accounts for the mechanical susceptibility of the lever in the frequency domain (*i.e*, force to position transfer function).

The motion sensor and various following electronic elements of the detection system incorporate some additional noises $w$ on the lever position. Finally the measurement $y$ can be expressed as :

$$y = z + z_n + w \tag{3}$$

Figure 2 illustrates typical force noise density that can be acquired with the Atomic Force Microscope used in experiments presented in this paper. It consists of detection noise $w$, which forms a background at a value around 1 $pm^2/Hz$, and thermo mechanical noise $z_n$ which has a peak dominant around the resonance frequency $\omega_r$.

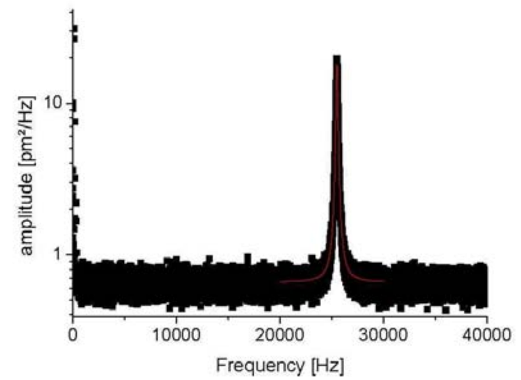


Fig. 2. Noise spectral density on Asylum MFP 3D Atomic Force Microscope, at room temperature.

The main purpose in this context is to recover as closely as possible the interaction force $F$ from direct measurement $y$.

## III. Proposed observer approach

In view of the previous problem formulation, the point here is to summarize how a solution can be obtained via observer techniques. This provides an alternative approach to the most common use of AFM devices.
It can be noticed that such an approach can already be found in few recent references, either with the idea to reconstruct $z, \dot{z}$ and from this detect $F$ (as in [Sahoo et al.(2005)Sahoo, Sebastian, and Salapaka]), or with the purpose of direct reconstruction of $F$ together with $z$ and $\dot{z}$ (as in [Besançon et al.(2004)Besançon, Voda, and Chevrier], [Besançon et al.(2007)Besançon, Voda, and Chevrier]).
In the present paper, we will focus on this second approach, and illustrate its performances on actual experimentations, in the continuity of those former formal suggestions.
In short, the idea consists in neglecting the force dynamics, either because the considered force is indeed not varying, or because its reconstruction will be fast enough. In both cases, this means that $F$ can be assumed to satisfy: $\dot{F} = 0$.
Then variables $z, \dot{z}$ and $F$ of basic equation (1) can be considered as state variables of a vector $x$, for a state space representation only driven by thermo-mechanical noise $f_n$ on the one hand, and detection noise $w$ on the other hand, as follows:

$$\begin{aligned} \dot{x} &= \begin{pmatrix} 0 & 1 & 0 \\ \frac{-k}{m} & -\frac{f}{m} & \frac{1}{m} \\ 0 & 0 & 0 \end{pmatrix} x + \begin{pmatrix} 0 \\ \frac{1}{m} \\ 0 \end{pmatrix} f_n \\ &:= Ax + Df_n \\ y &= \begin{pmatrix} 1 & 0 & 0 \end{pmatrix} x + w \\ &:= Cx + w \end{aligned} \quad (4)$$

On this basis, $(A, C)$ clearly being observable, a standard state observer can be designed in order to recover all state variables, namely an observer of the form:

$$\dot{\hat{x}} = A\hat{x} - K(C\hat{x} - y) \quad (5)$$

where $K$ is to be appropriately chosen.
In a deterministic framework, it can be chosen according to any pre-specified set of observer poles, but with no guarantee w.r.t. the noises. In a stochastic framework instead, the well-known *Kalman observer* provides an optimal choice for $K$, in the sense of minimizing the mathematical expectation $E[(\hat{x}(t) - x(t))^T(\hat{x}(t) - x(t))]$. This can be done provided that noise variances are known and used in the gain computation. However, it can be noticed that an admissible constant gain can be obtained in this context *only if* $(A, D)$ *is stabilizable*, which is not true in (4).
In practise, $D$ can be changed into $\begin{pmatrix} 0 & 0 \\ \frac{1}{m} & 0 \\ 0 & \varepsilon \end{pmatrix}$ for some $\varepsilon$ to be chosen, assuming some additional possible fluctuations in the force profile.
Then by playing on this parameter $\varepsilon$ for instance, one can tune the observer convergence rate w.r.t. the noise attenuation.
This observer approach has been tested on the experimental set-up proposed for this purpose, as described in previous section. In practise, the force to be reconstructed is simulated via an electrostatic action, driven by a voltage which can be used as a reference. For this reason, the observer performance will be rather validated by voltage estimation, relying on a force model w.r.t. this voltage, injected in model (4).
Some experimental results in that respect are reported in next section.

## IV. Experimental application and validation of the proposed observer strategy

In order to experimentally validate the proposed force measurement approach, in figure 1, a controlled voltage $V$ is introduced between the tip and the sample so as to produce an electrostatic force. In this way, the setup here described makes it possible to monitor non contact force applied on the lever. The corresponding model between the tip and the force (4) has thus been experimentally identified, and a corresponding observer (5) has been designed.

### *A. Identification of microlever physical parameters*

The experiment is carried out with an Asylum MFP-3D microscope. As shown in Fig. 1, a microlever is brought within about 1 $\mu$m from a gold flat surface. It corresponds to model Mikromash CSC37 Ti-Pt lever B, and has be chosen for its low stiffness ($k$=0.4 N/m) and for the conductive layer coated on it.

The microlever and the surface are forming a capacitance $C(d)$, that depends on the distance between them $d$. When applying a bias voltage $V$, an electrostatic force $F_e$, that is attractive, arises on the probe. It is described by:

$$F_e = \frac{1}{2} C' V^2 \quad (6)$$

where $C'$ is the capacitance derivative with respect to tip sample distance $d$. As a result, tuning the bias $V$ makes it possible to easily monitor the force intensity. As explained in section II, the probe is described as an harmonic oscillator with mass $m$, stiffness $k$ and damping coefficient $f$. It should be noticed that those parameters depend on how the force $F_e$ is applied. Resonance frequency $\omega_r = \sqrt{k/m}$ and damping rate $\gamma = f/m$ remain nevertheless the same: they can be identified from motion noise spectral density or force tuning diagram.

In the frequency domain, the mechanical response is thus described by:

$$H(\omega) = \frac{Z}{F} = \frac{1}{m({\omega_r}^2 - \omega^2 + j\gamma\omega)} \quad (7)$$

Motion detection calibration is performed using force-distance curve, that consists in putting into contact the tip with the sample surface and in extending the sample stage piezo translator $Z$ towards it: the microlever deflection is then equal to the piezo translator extension. Sensitivity $\alpha = Z/V_p$ is estimated at 188 nm/V (in the range 100-200 nm/V or the corresponding value), where $V_p$ is the voltage delivered by the photodiode in figure 1.

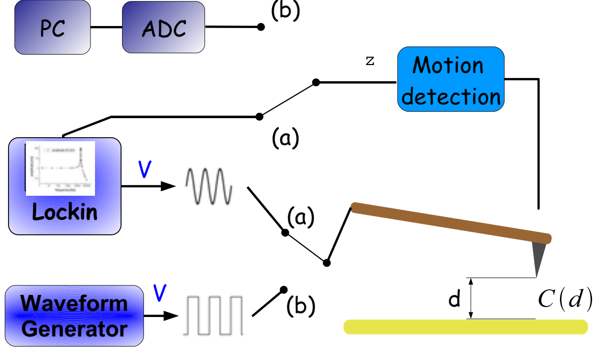


Fig. 3. Experimental configurations. Connection (a) is used for mechanical response acquisition through the lockin. Connection (b) enables the force acquisition to be recorded through an ADC linked to a PC.

In our experiment, it appears more convenient to reconstruct directly bias voltage $V$ than force $F_e$, so that its estimation ($\hat{V}$) can be directly compared to the "reference" $V$.
In order to implement an observer-based method, the response $G(\omega) = Z/V^2$ has rather to be identified. Using Eq. (6) and Eq. (7), it follows:

$$G(\omega) = \frac{C'}{2m} \frac{1}{\omega_r{}^2 - \omega^2 + j\gamma\omega} \tag{8}$$

Flowchart (a) of Fig. 3 describes the experimental setup. A sinusoidal shape voltage $V = V_0 \sin(\omega t)$ is put between the tip and the sample, thus generating an electrostatic force $F_e$ proportional to $V^2$.

$$V^2 = V_0^2 \frac{1 - \cos(2\omega t)}{2} \tag{9}$$

The $2\omega$ frequency component is scanned from 1 Hz to 100 kHz and then demodulated by a lockin amplifier. The mechanical response is finally plotted and compared to that obtained with model (8) in Fig. 5. Fitting parameters of Eq. (8) are found to be given by:

$$\begin{aligned} \omega_r &= 1.5215 \times 10^5 rad/s \\ \gamma &= 1570 rad/s, \\ \frac{C'}{2m} &= 1.27 \times 10^9 nm.s^2/V^2 \end{aligned}$$

The discrepancy between data and model is lower than 5 % (and could be reduced by introducing mechanical response background associated to higher vibration modes). As a result, this analysis validates the damped harmonic oscillator as the model that well captures the microlever mechanical behavior.
The resulting model can then be re-written as (4) and used for observer design.
The corresponding electrostatic force measurements are carried out following flowchart (b) of Fig.3. Rectangular shape voltages are applied on the tip, thus causing the lever to deflect as shown in Fig. 4. An Analog Digital Converter (ADC) samples the microlever motion signal at 1 MHz.

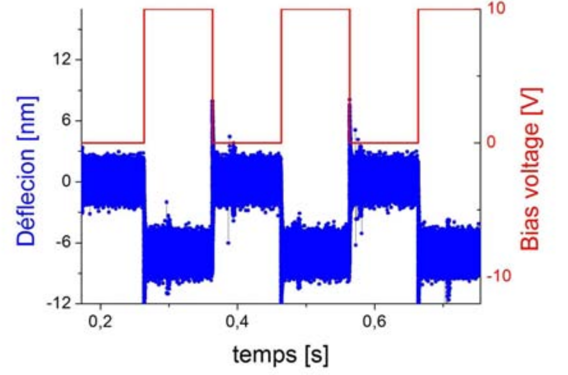


Fig. 4. Typical cantilever deflection (bottom) versus bias voltage (top), on Asylum MFP 3D Atomic Force Microscope, using a cantilever Mikromash CSC37 Ti-Pt lever B.

The deflection signal is here disturbed by noises, mechanical resonance phenomenon and various drift (mechanical or electrical). However, the latter are here neglected because measurement time is small.

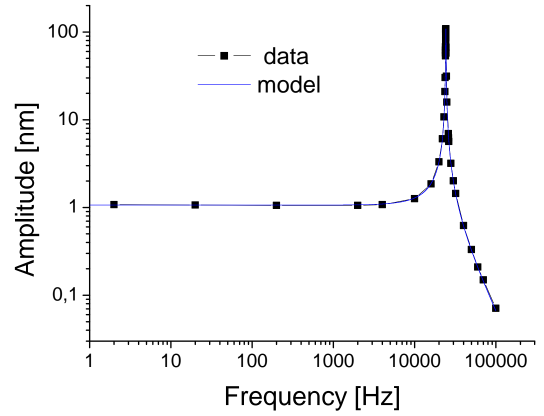


Fig. 5. Mechanical response of the lever, on Asylum MFP 3D Atomic Force Microscope, using a cantilever Mikromash CSC37 Ti-Pt lever B.

### B. *Observer-based force reconstruction*

Let us present now some observation results obtained in the context previously described. Two cases will be more particularly discussed: a low frequency problem on the one hand, and some higher frequency case on the other hand.

*1) Step change of the force:* The first experiment reported here thus corresponds to a single step change in the applied voltage, resulting in a transient response of the cantilever presented in figure 6.

On this basis, an observer can be designed which achieves a very good noise filtering in a few milliseconds, as illustrated by the voltage reconstruction shown on figure 7.
Notice that this corresponds to the estimation of a force with a magnitude of few nanoNewtons.

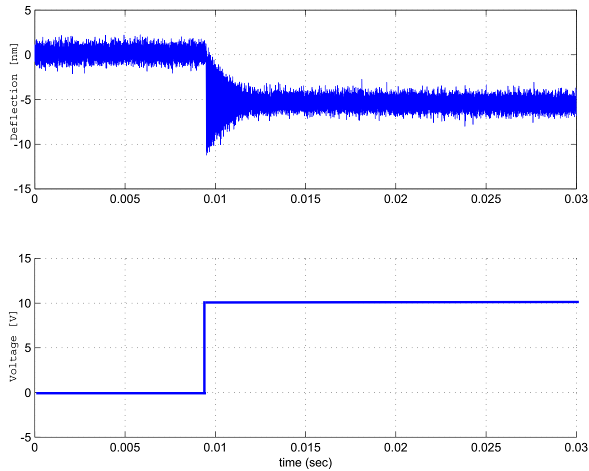


Fig. 6. Measured cantilever deflection (top) vs applied voltage (bottom) - step case. Asylum MFP 3D Atomic Force Microscope is used.

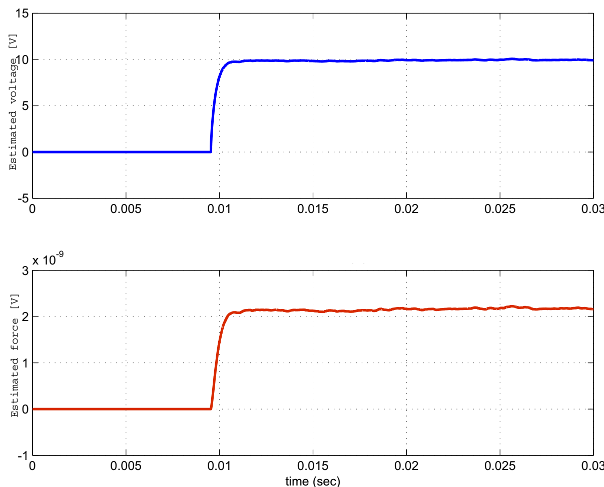


Fig. 7. Observer-based estimated voltage (top) and estimated force (bottom) - step case. Asylum MFP 3D Atomic Force Microscope is used.

*2) Fast step change of the force:* In case of faster force variations (here voltage variations), for instance up to $1kHz$ step variations - as considered for a second experiment, this observer will be limited.
A faster one can yet be designed, still achieving a fairly good voltage (and force) reconstruction.

## V. Conclusion

In this paper a full observer approach towards force measurement from AFM collected data has been developed, including a specific AFM set-up description for such an approach, the corresponding model identification, and some possible (Kalman) observer design. This methodology is illustrated by very promising experimental results, and will be pushed forwards in future developments.

## References

[Albrecht et al.(1991)Albrecht, Grütter, Horne, and Rugar] T.R. Albrecht, P. Grütter, D. Horne, and D. Rugar. Frequency modulation detection using high-Q cantilevers for enhanced force microscope sensitivity. *Journal Applied Physics*, 69(2):668–702, 1991.

[Besançon et al.(2004)Besançon, Voda, and Chevrier] G. Besançon, A. Voda, and J. Chevrier. Force estimation in fundamental physics: an observer application. In *2nd Symp. on System Structure and Control, Oaxaca, Mexico*, 2004.

[Besançon et al.(2007)Besançon, Voda, and Chevrier] G. Besançon, A. Voda, and J. Chevrier. An observer for nanoforce estimation with thermal noise attenuation. In *Proceedings of Conference on Systems and Control, Marrakech, Morocco*, 2007.

[Binnig et al.(1986)Binnig, Quate, and Gerber] G. Binnig, C.F. Quate, and C. Gerber. Atomic force microscopy. *Physics Review Letters*, 56:930–933, 1986.

[Cleland(2004)] A.N. Cleland. *Foundations of Nanomechanics*. Springer, 2004.

[Clough and Penzien(1993)] R. W. Clough and J. Penzien. *Dynamics of Structures*. Mcgraw-Hill, 1993.

[García and Pérez(2002)] R. García and R. Pérez. Dynamic atomic force microscopy methods. *Surface science reports*, 47:197–301, 2002.

[Giessibl(2003)] F. Giessibl. Advances in atomic force microscopy. *Reviews of Modern Physics*, 75:949–983, 2003.

[Kwakernaak and Sivan(1972)] H. Kwakernaak and R. Sivan. *Linear optimal control systems*. Wiley-Interscience, 1972.

[Sahoo et al.(2005)Sahoo, Sebastian, and Salapaka] D.R. Sahoo, A. Sebastian, and M.V. Salapaka. Harnessing the transient signals in atomic force microscopy. *Int. J. Robust Nonlinear Control*, 15:805–20, 2005.

# A Mechanism Approach for Enhancing the Dynamic Range and Linearity of MEMS Optical Force Sensing

Gloria J. Wiens

***Abstract*—Optical based force sensors can provide the desired resolution and maintain relatively large sensing ranges for cell manipulation and microneedle injections via a force sensing method that uncouples the conflicting design parameters such as sensitivity and linearity. Presented here is a mechanism approach for enhancing the performance of a surface micromachined optical force sensor. A new design is presented which introduces a special mechanism, known as the Robert's mechanism, as an alternate means in which the device is structurally supported. The new design's implementation is achievable using an equivalent compliant mechanism. Initially, an analytical set of pseudo-rigid-body-model equations were developed to model the compliant design. A more accurate model was then constructed using FEA methods. The geometric parameters of the compliant Robert's mechanism were then optimized to obtain a sensor with improved linearity and sensitivity. Overall, the force sensor provides higher sensitivity, larger dynamic range and higher linearity compared to a similar optical force sensor that uses a simple structural supporting scheme. In summary, the effectiveness of using a mechanism approach for enhancing the performance of MEMS sensors is demonstrated. The expected impact is to improve biomedical experiments and help further advance research that can improve quality of life.**

## I. INTRODUCTION

A wealth of research has been conducted in microelectromechanical systems (MEMS) to develop physical sensors and actuators. As a consequence, MEMS technology has provided great advances in the area of force sensing. The miniaturization has allowed sensors to be packaged in sub-cubic millimeter volumes. This opened the door for the placement of sensors in previously impossible situations and locations. For diverse areas in biomedical research and clinical medicine, the versatility of micro-sensors and actuators is enabling ever-greater functionality and cost reduction in smaller devices for improved medical diagnostics and therapies.

A conventional force sensor was developed by Zhang *et al.* [1]. The sensor is integrated with a microneedle to be able to measure injection forces. It is a 1 DOF sensor using a linear optical encoder. The authors of [1] report a resolution of less than 1 $\mu N$ and a range of about 10 $\mu N$. The general operating principle of this device is common to many force sensors. That is they measure the displacement of a compliant structure with a known stiffness and calculate the force required to induce that displacement. Where these force sensors vary is the detection scheme employed to determine the displacement. Another common method is capacitive sensing. Sun *et al.* [2] have developed a capacitive force sensor to measure forces up to 490 $\mu N$ with a resolution of 0.01 $\mu N$ in $x$, and up to 900 $\mu N$ with a resolution of 0.24 $\mu N$ in $y$.

Both of these devices use simple compliant beams to support the sensing element of the sensor. There have been attempts to use more complicated compliant mechanisms in place of simple beams to improve sensor characteristics, such as linearity, resolution and dynamic range [3-6]. A compliant mechanism, termed "XBob", was developed in [7] using a combination of Robert's mechanisms to achieve straight-line motion. Presented herein, a compliant mechanism comprised of Robert's mechanisms is introduced as a design basis for replacing the simple beams in the above device of Zhang. An optimization was conducted to improve the performance characteristics of the sensor.

Manuscript received March 5, 2010. This work was supported in part by the GEM Fellowship Program. U.S. Patent Application No. 60/885,304 filed May 20, 2009.

G.J. Wiens is with the University of Florida, Gainesville, FL 32611 USA (phone: 352-392-0806; e-mail: gwiens@ ufl.edu).

## II. ENHANCEMENT OF OPTICAL FORCE SENSOR

### A. *Prior Art: Optical Force Sensor*

The MEMS force sensor presented in [1] was fabricated using a surface micromachining process at the Stanford Nano-fabrication Laboratory. The device is an optical force sensor based on a diffractive linear encoder. It consists of two constant period gratings. The scale grating is fixed to the substrate, while the index grating is suspended above the fixed grating by four beams. The two gratings are in alignment when no external force is applied to the index grating. For the purpose of characterizing microinjection forces, a microinjection needle is monolithically incorporated into the index grating. Any force applied to the needle causes the index grating to displace. Given a minimum detectable displacement, defined by the optics and photodiodes, the spring constant determines the sensitivity of the sensor. The more compliant the sensor, the smaller the minimum changes in force it may register.

The index grating supported by four beams was modeled as having two beams that pass through the index grating which act as springs. The beams act in parallel, therefore the equivalent spring constant of one beam may be determined and multiplied times two to give the overall spring constant of the force sensor. The boundary conditions of the beam

are set up as both ends fixed and center loaded. The fixed ends are anchored to the substrate and the index grating displacement is equivalent to the center applied load displacement. Using the optics to precisely determine displacement and the calculated spring constant, the magnitude of the force acting on the sensor can be found. For small tip deflections, bending is the dominating mode and the relationship between force and displacement can be considered linear. The linear operating range for this sensor is about 12 $\mu m$. These results were obtained using a 2-D non-linear elastic finite element analysis (FEA) model generated using ANSYS® software.

### B. *Compliant Mechanism Enhancement*

Using a mechanism approach to enhance the dynamic range and linearity of the sensor, a compliant mechanism is used in place of the simple beams to support the index grating of the prior sensor design. The compliant mechanism is based on a Robert's four-bar mechanism, shown in Figure 1. Using a design that Hubbard *et al.* [7] conceived of, a total of eight Robert's mechanisms are combined to form a new special mechanism with straight-line motion characteristics. A 3D model of the top layer of device is shown in Figure 2.

*1) PRBM Modeling:* The Pseudo-Rigid-Body-Model (PRBM) is a concept used to model the force-displacement relationships of a compliant member using an equivalent rigid-body mechanism with the compliance modeled as springs in the joints [7]. For the compliant model, the flexible segments are considered to have boundary conditions: fixed where attached to the ground or index grating and fixed-guided where attached to the middle rigid member as depicted in Figure 3.

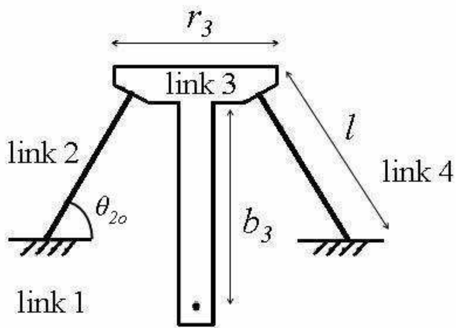


Fig. 1. A compliant version of the Robert's mechanism.

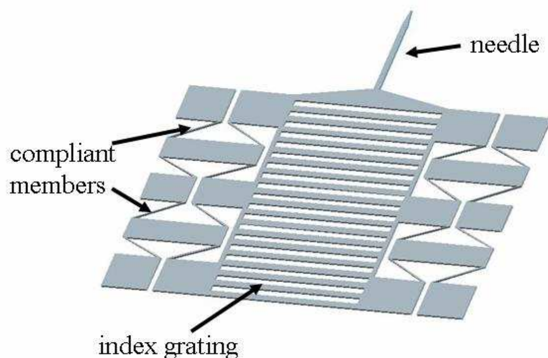


Fig. 2. Solid 3D model of final design: top nitride layer shown (not to scale).

*2) FEA Modeling:* A finite element analysis (FEA) is conducted to validate the PRBM model. The FEA also captures any nonlinear phenomenon that may occur, which is not possible using the PRBM alone. The model used in the FEA is shown in Figures 4 and 5. All beam elements not representing compliant members were given a larger width (20 $\mu m$) than the flexible links so that they would exhibit rigid behavior compared to the flexible links. The same value of 270 *GPa* was used for the Young's modulus and 0.24 for Poisson's ratio. All force-displacement curves were generated by a static analysis of 10 equivalently spaced displacement load steps. In order to verify that 10 load steps provided enough data points for accurate results, a test case was run. The test case held everything constant and ran the simulation with 50 load steps and 10 load steps. It was found that the selection of 10 data points did not omit any significant trends when compared to the 50 load step case. The displacement input was applied to the center of the rigid section, which represents the index grating. The reaction force at all fixed nodes were tabulated for each load step.

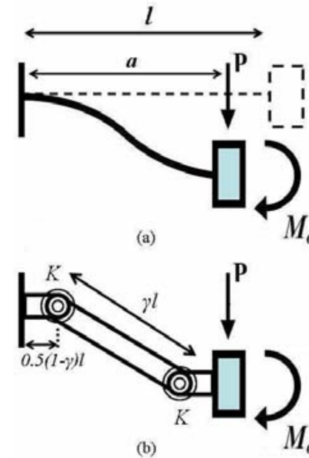


Fig. 3. Fixed-guided beam: (a) flexible member, (b) pseudo-rigid body model equivalent.

### C. *Design Optimization*

For this device, nitride is the material of choice due to its optical properties. The thickness of the nitride is also pre-selected to achieve desirable optical properties. This leaves the length of the links, the initial angle of the link 2, and the width of the compliant member as available design variables for parameter optimization. For the design optimization, the objective function was selected to maximize full scale linearity and minimize the overall stiffness, subject to constraints and boundaries. This is a dual objective problem where initially each objective was weighted equally ($\alpha$ = 0.5). This can be stated mathematically as follows:

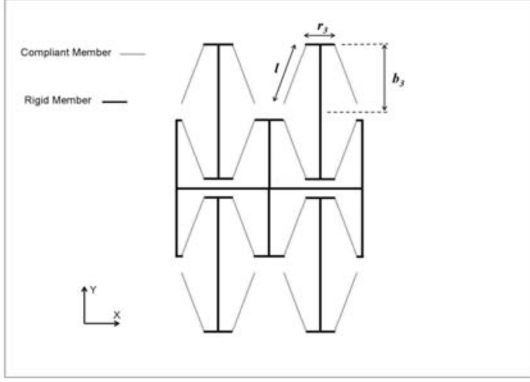


Fig. 4. Finite element 2D model of compliant mechanism in unloaded state.

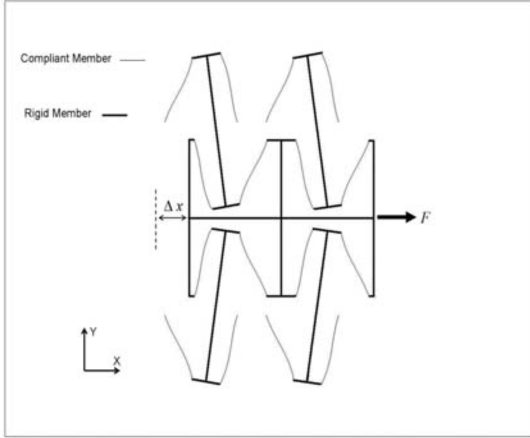


Fig. 5. Finite element 2D model of compliant mechanism

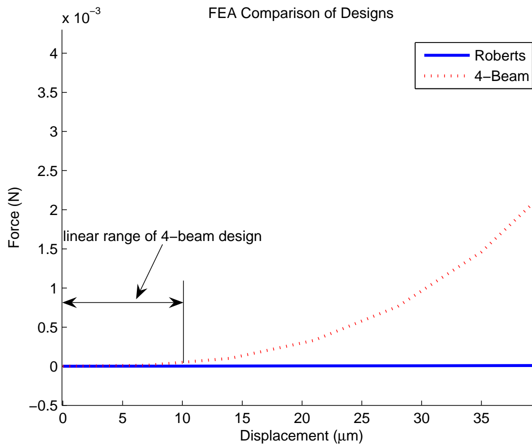


Fig. 6. Comparison of FEA results for Robert's and 4-beam designs.

$$(\alpha)\min k_{sensor} \quad \& \quad (1-\alpha)\max linearity :\rightarrow f(w,l,r_3,b_3,\theta_{2o})$$
$$l, r_3, b_3 \in [1\mu m, 300\mu m]$$
$$w \in [1\mu m, 10\mu m]$$
$$\theta_{2o} \in \left[20^\circ, 90^\circ\right]$$

The lower bound of 1 $\mu m$ was placed on all length and width variables because this is a minimum feature size that can be fabricated using most common surface micromachining. The upper bound on the link lengths was set to keep the design within a practical size footprint; something comparable to the current force sensor. Therefore a value of 300 $\mu m$ was selected. The upper bound of the width was also selected somewhat arbitrarily. However, it must remain within the restraints that require these links to exhibit compliant behavior relative to the adjacent rigid links.

To prevent the optimization from yielding impractical designs, the initial angle $\theta_{2o}$ was constrained so that resulting configurations would exhibit geometries that would not interfere with the index grating and would yield desirable link 2 orientations. Initially, the domain for $\theta_{2o}$ was from 0° to 90°. Configurations with angles below 20° did not violate any of the specified constraints, but did cause errors for the FEA simulation. Configurations with angles in this range resulted in mechanisms with force-displacement relationships that could not be handled by the FEA nonlinear solver. For this reason the lower bound on $\theta_{2o}$ was raised to 20°. Another constraint declares that the configurations must not violate any physical kinematic constraints. In particular, a constraint is introduced that prevents links from occupying the same space at the same time and prevents any binding or interference.

## III. Design Results

The results of the PRBM and FEA analysis and design optimization show a vast improvement which becomes apparent when the force-displacement curves are plotted together, as in Figure 6. In the design of the 4-beam sensor, nonlinearities begin to dominate after only 15 $\mu m$ of displacement. The new Robert's design remains virtually linear throughout the entire displacement range (in plot of Figure 6 it appears to be a horizontal line due to the scale of the nonlinearities of the 4-bar sensor). Therefore the force can be simply calculated using the pre-determined spring constant and computed displacement. Based on the analysis presented, the force values obtained with the new design will be accurate over the specified full range of motion. The 4-beam design will only exhibit a linear relationship if the sensor operates up to 10 $\mu m$, after which the sensor will be producing erroneous force values or would require nonlinear calibration curves.

## IV. Summary and Conclusions

This work demonstrated the effectiveness of using a mechanism approach for enhancing the performance of a MEMS sensor. The work entailed the re-design of a surface micromachined optical force sensor. The sensor uses an optical diffraction sensing scheme to resolve forces induced from input displacements. This device is geared toward cell manipulation and microinjection. Focusing on the structural support elements of the sensor, a Robert's mechanism was selected to replace the current simple beam structure. The Robert's mechanism was chosen because of its linear motion and force characteristics. This mechanism was combined in series and parallel to form another mechanism with desirable traits. The geometric parameters of the Robert's mechanism were optimized to obtain a sensor with improved linearity and sensitivity. The presented techniques from this research could also be used to pursue designs for other applications. The Robert's mechanism is designed to be implemented as a compliant mechanism. This allows the sensor to be monolithically fabricated via surface micromachining and bulk etching technologies.

## References


[1] X. Zhang, S. Zappe, R. Berstein, O. Sahin, C. Chen, M. Fish, M. Scott, and O. Solgaard, "Micromachined silicon force sensor based on diffractive optical encoders for characterization of microinjection," *Sensors and Actuators: A Physical*, **114**(2-3), 2004, pp. 197–203.

[2] Y. Sun, B. Nelson, D. Potasek, and E. Enikov, "A bulk-fabricated multi-axis capacitive cellular force sensor using transverse comb drives," *J. Micromechanics and Microengineering*, **12**, 2002, pp. 832–840.

[3] A. Sexena, and G. Ananthasuresh, "Optimal property of compliant topologies," *Struct. Multidiscip. Optimization*, **19**(1), 2000, pp. 36-49.

[4] C. Pedersen, and A. Sechia, "On the optimization of compliant force amplifier mechanisms for surface micromachined resonant accelerometers," *J. Micromech. Microeng.*, **14**, 2004, pp. 1281-1293.

[5] J. Wittwer, T. Gomm and L. Howell, "Surface micromachined force gauges: uncertainty and reliability," *J. Micromech. Microeng*. **12**(1), 2002, pp. 13-20.

[6] X. Wang, and G.Ananthasuresh, "Visiion-based sensing of forces in elastic objects," *Sensors and Actuators: A Physical*, **94**(3), 2001, pp. 142-156.

[7] N. Hubbard, J. Wittwer, J. Kennedy, D. Wilcox, and L. Howell, "A novel fully compliant planar linear-motion mechanism." *Proc. of the 2004 ASME Design Engineering Technical Conferences*, Salt Lake City, Utah, DETC2004-57008, 2004.